Psyrras, N., & Sextos, A. (2018). Safety of buried steel natural gas pipelines under earthquake-induced ground shaking: a review. *Soil Dynamics and Earthquake Engineering*, *106*, 254-277. https://doi.org/10.1016/j.soildyn.2017.12.020

Safety of buried steel natural gas pipelines under earthquake-induced ground shaking: a review

Nikolaos K. Psyrras[1] and Anastasios G. Sextos[2]

Abstract. Evidence from past earthquakes suggests that damage inflicted to buried natural gas (NG) pipelines can cause long service disruptions, leading to unpredictably high socioeconomic losses in unprepared communities. In this review paper, we aim to critically revisit recent progress in the demanding field of seismic analysis, design and resilience assessment of buried steel NG pipelines. For this purpose, the existing literature and code provisions are surveyed and discussed while challenges and gaps are identified from a research, industrial and legislative perspective. It is underscored that, in contrast to common belief, transient ground deformations in non-uniform sites are not necessarily negligible and can induce undesirable deformations in the pipe, overlooked in the present standards of practice. It is further highlighted that the current seismic fragility framework is rich in empirical fragility relations but lacks analytical and experimental foundations that would permit the reliable assessment of the different parameters affecting the expected pipe damage rates. Pipeline network resilience is still in a developing stage, thus only few assessment methodologies are available whereas absent is a holistic approach to support informed decision-making towards the necessary mitigation measures. Nevertheless, there is ground for improvement by adapting existing knowledge from research on other types of lifeline networks, such as transportation networks. All above aspects are discussed and directions for future research are provided.

Keywords. Buried pipeline; natural gas; seismic resilience; gas networks; service disruption; seismic fragility; soil-pipe interaction; structural health monitoring

[1] Ph.D. Candidate, Department of Civil Engineering, University of Bristol, United Kingdom
[2] Assoc. Professor, Department of Civil Engineering, University of Bristol, United Kingdom

1 INTRODUCTION

Natural gas (NG) is nowadays a cornerstone in supplying energy to industry and households, maintaining an important share in the global energy market. A steadily growing dependence of the global energy demand on NG is reflected in numbers: one quarter of the total energy demand in the US and the European Union is currently satisfied by NG delivery [1], while it is projected that by 2040 nearly one quarter of the global electricity will be generated by NG [2]. Extensive onshore networks of buried steel pipelines are the method of choice for inland NG distribution from wells to end-users, with steel being used almost exclusively for the large-diameter transmission network. For further details on NG pipeline technology, the interested reader is referred to Folga [3].

However, of the heaviest dependents on NG are earthquake-prone regions, such as California in the United States, south-eastern Europe (Italy, Greece, Turkey and the Balkans), Japan and New Zealand, which are all exposed to significant seismic hazard. Experience from past earthquakes has repeatedly demonstrated that buried pipelines are vulnerable to seismic effects. In line with existing literature, these seismic effects can be divided into two main groups of 'geohazards', based on the temporal nature of the damage source: (a) transient ground deformation (*TGD*) due to seismic wave propagation, and (b) permanent ground deformation (*PGD*), with possible failure causes being active fault movements, landslides, liquefaction-induced settlement or lateral spreading (Figure 1). Most of the damage reported to date is attributed to PGD [4,5], but there is also strong evidence that wave propagation has contributed to pipe damage [6–12], though to a lesser extent.

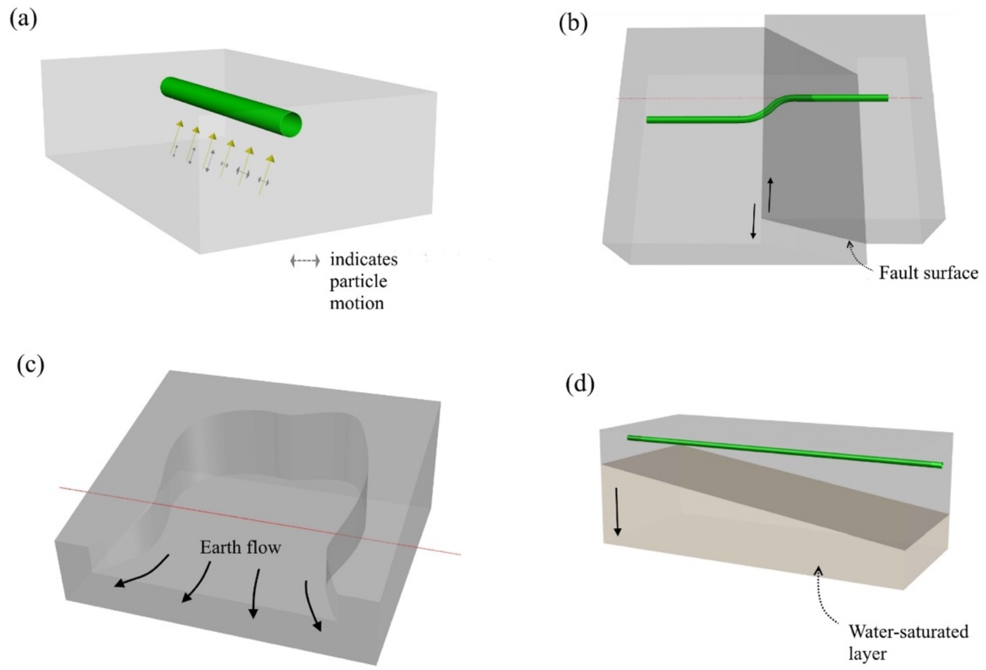

Fig. 1. Illustration of the major geohazards threatening the structural integrity of buried NG pipelines: (a) seismic wave propagation; (b) – (d) PGD types: (b) strike-slip fault movement; (c) landslide in the form of earth flow; (d) liquefaction-induced settlement.

From a system-wide viewpoint, the impact of a seismic shock on the network level of a NG pipeline system can be highly adverse and spatially dispersed. A potential long-lasting flow disruption due to earthquake damage can have excessive direct and indirect socioeconomic repercussions not only locally, but also internationally, given the spatial dimension of a NG network. Records on the number of NG network users that experienced service disruption and the disruption duration after past earthquake events can be found in relevant reports [5,7,12,13]. Additionally, content leakage may have life-threatening consequences if ignition is triggered and can pose an environmental threat. It becomes therefore evident that underground NG networks traversing seismically active areas are exposed to seismic risk and, consequently, securing their long-term integrity and operability with the minimum cost to society and economy is of paramount importance. This very objective has given rise to the concept of *resilience* in recent years, which is commonly perceived as the capacity to cope with unanticipated dangers after they have become manifest, learning to bounce back, or the ability to resist, adapt to and recover from some shock, insult or disturbance. As resilience is of paramount importance for all lifeline systems, strategies for improvement are gradually being adopted as a desired target by authorities and influential movements within policy-making for natural disaster mitigation in urban environments.

Given the above challenges, the objectives of the present review study are to:

a) Identify and examine one by one essential aspects pertaining to the seismic safety of buried steel NG pipelines, both on the component and the network level. These aspects are identified by the section titles following,
b) For each element of this analysis, point out and discuss the most important outcomes and conclusions found in the literature that relate to the way we design and assess NG buried pipeline networks in seismogenic regions,
c) Highlight the primary challenges involved in each subdomain in light of the latest knowledge and pinpoint limitations and gaps that need to be filled by new research.

Analyze interrelationships among the different elements, where possible and discuss ideas for possible future research work, more so towards an integrated seismic resilience assessment framework.

The novelty herein lies in the fact that we attempt to approach the most critical aspects of seismic safety of buried NG pipelines in a holistic manner. Previous similar efforts on pipelines (e.g. [14–17]) or with a broader structural typology scope [18,19] dealt only with specific aspects independently of one another, such as response analysis and design or fragility analysis. It must be emphasized that the scope is focused on TGD effects. The reasons are that TGD involves more complex physics and more uncertainties, it is statistically more likely to affect buried pipelines due to its spatially distributed character, it is not as well documented as PGD cases and, in contrast to the above, it is often overlooked. On the other hand, pipelines under PGD is a well-developed topic supported by a large volume of analytical and experimental studies, especially in recent years. However, throughout this text, references to research explicitly dealing with PGD are also made, because these two seemingly different types of ground movement (TGD and PGD) share some common characteristics, as explained later. References to some studies on water mains are also made when the material used is steel to provide a better insight in the phenomena studied.

The structure of the study is as follows. First, five interlinked aspects of seismic safety of buried NG pipelines are reviewed in detail in a bottom-up order, starting with component and ending with network features, namely: (a) governing failure mechanisms and relevant field observations; (b) pipe response analysis elements, including soil-pipe interaction (SPI), spatial variation of seismic ground motion along the pipeline and applicable analysis methodologies; (c) seismic vulnerability of NG pipelines; (d) structural health monitoring; and (e) seismic resilience at the network level. Then, existing seismic code provisions for pipeline design are critically assessed to determine to which extent they address the latest research findings. Finally, unaddressed issues are outlined and discussed altogether, and suggestions are made for future research and improvement of existing codes.

2 DOMINANT FAILURE MODES AND ASSOCIATED CRITERIA

In the course of earthquake-resistant design of underground steel pipeline networks, one has to first identify the principal mechanisms leading to pipe failure due to seismic excitation in order to establish appropriate performance criteria and select effective analysis methodologies. Extensive previous research efforts and field surveys have been successful in classifying the most frequently occurring failure modes into two main groups: those prevalent in continuous and those usually observed in segmented pipelines. The first group includes line pipes assembled with welding techniques, the welds being equally strong or stronger than the pipe barrels themselves [3]. The second group includes pipelines in which connections are achieved by means of mechanical joints, which are the weak link of the chain due to their lower strength. Herein, discussion is restricted to continuous pipelines, because they are preferred for NG networks. One can distinguish five common damage states for continuous steel-welded pipelines triggered by ground deformation: (i) shell-mode buckling, (ii) beam-mode buckling, (iii) pure tensile rupture, (iv) flexural failure, and (v) section ovalization [20,21] as shown in Figure 2. Each one is discussed in detail in this section.

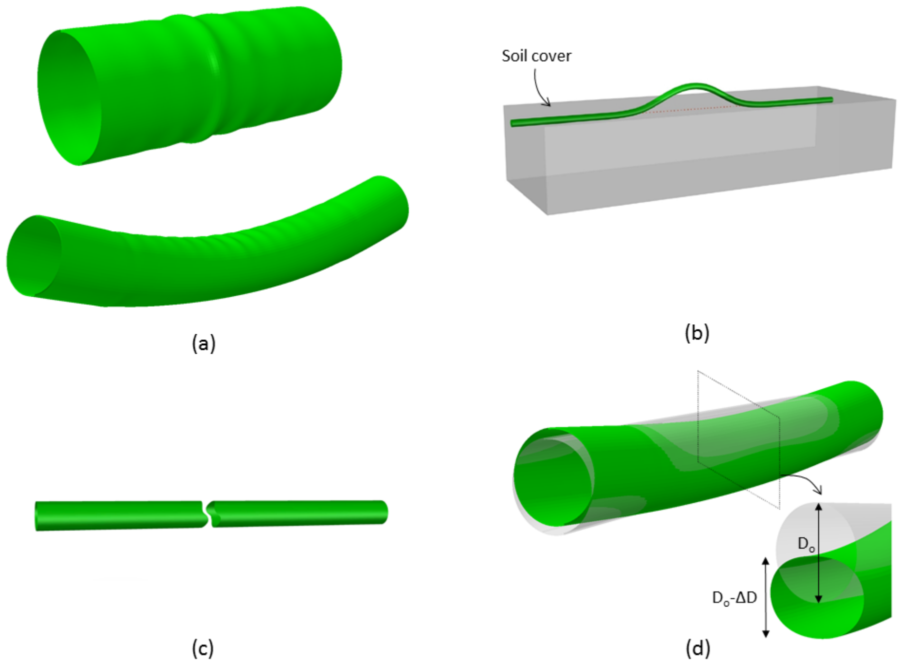

Fig. 2. Common failure mechanisms in buried, continuous steel pipelines: (a) shell-mode buckling due to uniform axial compression (top) and pure bending (bottom); (b) beam-mode buckling; (c) tensile fracture and (d) cross-section ovalization.

2.1 Shell-mode buckling

Shell-mode (also referred to as local) buckling is a failure condition associated with loss of stability arising under compressive load or bending moment. Typical radius to thickness (R/t) ratios (e.g. R/t <33 for a safety factor of 2 for pressure loading) and steel grades (σ_y >350 MPa) used in NG pipeline applications dictate that shell-mode instabilities are expected in the inelastic range of response, both for axial and bending loading [22]. Initial small deviations of the pipe walls from the perfect geometry can destabilize the nonlinear load-displacement path causing bifurcation of the deformation, manifesting itself as wall wrinkling. With increasing load, the stiffness gradually drops and these wrinkles will grow and start to localize, leading to a limit load instability or a secondary bifurcation, usually in a non-axisymmetric mode, depending on the plastic steel characteristics and the R/t ratio. The highly localized deformation may cause wall tearing and content leakage. Local buckling is a common failure mode in steel pipelines, as indicated by field observations of pipeline performance in past earthquakes [7,20]. Specifically, local buckling caused by TGD affected a water pipe during the 1985 Michoacan event in Mexico City, whilst liquid fuel, water and gas pipelines suffered such damage in the 1991 Costa Rica and 1994 Northridge earthquakes. Local buckling due to PGD was also evident in pipelines crossing faults, both normal and reverse, in the 1971 San Fernando event. Experience so far shows that wrinkling tends to initiate near geometric imperfections or discontinuities, such as elbows and girth welds [23]. It is also noted that particularly for the case of buried pipelines, non-uniform compaction of the subsoil within the trench may act as a potential imperfection of the pipe-soil system as it will be discussed later.

Elastic and inelastic buckling of standalone cylindrical shells is a well-established topic in the literature given the long identified problems in industrial applications. On the other hand, the buckling problem of shallow-buried cylindrical shells, which can be idealized as buckling under constraints (i.e., confinement by the surrounding soil), is not yet as mature. Chen *et al.* [24] and Lee *et al.* [25] used shell stability formulations to study the elastic static and dynamic elastoplastic axial buckling of a buried pipeline, respectively. Yun and Kyriakides [26] further provided vital insight into the parameters that control the occurrence of shell-over beam-mode (see Section 2.2) buckling in buried pipelines under seismically-induced axial compression. Their sensitivity analyses show qualitatively that combination of conditions such as large diameter, large *R/t* ratio and deep soil covers favour shell-mode buckling. Pipelines embedded in stiffer soils display a slight increase in the buckling loads and strains, but what exerts greater influence on the pipe response is the amplitude of the initial imperfections.

Hall and Newmark [27], based on previous experimental results, recommended a strain-based criterion for the onset of shell-type buckling in buried pipelines as a function of the reciprocal of *R/t* (adopted as a design provision by ASCE [28]):

$$0.15(t/R) \leq \varepsilon_{cr} \leq 0.20(t/R) \tag{1}$$

where ε_{cr} is the critical buckling strain. O'Rourke and Liu [20] note that the above criterion finds better applicability to thin-walled pipes, while it is rather conservative for thick-walled ones. In reality, most NG transmission pipelines lie in the intermediate range. Vazouras *et al.* [23] also establish a 'no-buckling' condition for buried pipelines deformed by strike-slip fault movement normal to their axis:

$$R/t \leq 0.05a(L/R)^2 \tag{2}$$

where L is the length of the deformed segment of the pipeline and a is a parameter depending on the pipeline material and initial imperfections.

2.2 Beam-mode buckling

Shallow-buried NG pipelines subject to compressive ground forces are also likely to suffer from beam-mode buckling (sometimes referred to as 'upheaval' buckling, but this term is only meaningful for vertical upward pipe motion), a failure mode that resembles the well-known Euler buckling of a column. In this failure mechanism, the pipeline is forced to bend upwards, where the soil resistance is lower, sometimes revealing itself out of the ground, as it has been witnessed in previous earthquakes. Because deformation localization is not as severe as in shell-mode buckling, the likelihood of pipe breakage is generally low, therefore beam-mode buckling is considered a less catastrophic failure mode [20]. That said, beam-mode buckling is better characterized as a serviceability peril, since the content flow is not necessarily interrupted. A limit state criterion for beam-mode buckling depends on several parameters, such as the flexural rigidity of the pipe section, potential imperfections and the burial depth of the pipeline. As such, it is challenging to be reliably quantified without experimental justification.

Observations from past earthquakes verify the occurrence of beam-mode buckling in some cases. In 1959, oil pipelines embedded in a shallow trench with a depth ranging between 0.15 and 0.30m and traversing the Buena Vista reverse fault, lifted out of the ground because of high compression stresses. In another interesting occasion related to the 1979 Imperial Valley seismic event, there was no evidence of upheaval buckling until local inspections by means of cover removal forced the pipelines to buckle upwards [29]. This is also an indication that beam-mode buckling may not always interrupt the functionality of the pipeline. Beam-mode buckling damage was also reported after the Niigataken Chuetsu-oki earthquake in Japan [30].

Again, Yun and Kyriakides [26] analysed the factors that contribute to beam-mode buckling failure. As anticipated, in pipelines with smaller diameters, smaller *R/t* ratios and shallower burial depth, beam-mode buckling tends to dominate. However, it was claimed that in the most realistic case, shell- and beam-mode buckling essentially interact; in fact, coupled axial compression and bending can produce localized deformation at buckling loads lower than the ones predicted for shell-buckling alone. Meyersohn and O'Rourke [31] noticed that pipelines covered by backfill soil with limited uplift resistance are more likely to fail by means of beam-mode buckling. They pointed out that there is a proportional relationship between buckling load and trench depth and calculated a critical value for the latter, which governs the precedence of occurrence of the two modes of buckling; that is, if a pipeline has a larger burial depth than the critical cover depth, then shell-mode buckling will occur before beam-mode buckling and vice versa. It was also noted that a minimum cover depth of 0.5 to 1.0m is sufficient to ensure that the pipeline will not experience beam-mode buckling.

More recently, Matheson and Zhu [32] carried out a parametric numerical study of an idealized buried pipeline model with hill-crest overbend imperfection under service loads, in order to establish an empirical formula and limit state for the critical upheaval buckling load. Wang *et al.* [33] set to determine the upward pipe displacement required to mobilize the upheaval buckling resistance by conducting full-scale plane-strain soil-pipe tests in order to avoid scaling law problems. It was found that mobilization distance relates linearly to the burial depth-to-diameter ratio. Mitsuya *et al.* [34] managed to reproduce the beam-mode buckling that occurred in buried pipelines during the Niigataken Chuetsu-oki earthquake by developing a simple formula that makes use of elastic stability theory and tangent modulus theory. The critical strain is given by:

$$\varepsilon_{cr} = \left(\frac{4k_{\ell} I}{A^2} \frac{\varepsilon_{0.2}^{n}}{\sigma_{0.2}} n \right)^{1/(n+1)} \tag{3}$$

where A is the pipe cross-sectional area, I its second moment of inertia, k_ℓ the lateral spring constant, $\sigma_{0.2}$ the 0.2% steel proof stress and $\varepsilon_{0.2}$ the corresponding strain, n stands for a work-hardening exponent.

2.3 Tensile rupture

When the pipeline is in a state of axial tension, rupture is expected to occur if excessive plastic longitudinal strains develop in the pipe walls. This type of failure is rarely observed in arc-welded steel pipelines with butt connections due to the strongly ductile behaviour of the latter. On the contrary, steel pipelines assembled with gas-welded slip joints are more vulnerable to this failure mechanism, since they are incapable of withstanding substantial yielding prior to rupture. This finding is described in [35], based on evidence from the 1994 Northridge event.

Although the ultimate strain of X-grade pipe steel may well reach 21% according to manufacturers' specifications [36], usually a more conservative value of 2%, 3% [37,38] or 4% [20] is adopted in engineering practice and research. However, there is a debate on whether these values are representative of the real ductility capacity of steel at the weakest locations of a steel-welded pipeline: girth welds and potential wall defects (elaborated in Section 3.4). Girth welds, although designed with higher strength provisions than the pipe barrels [3], may exhibit lower ductility than the nominal value owing to metallurgical alterations induced by the welding process. Considering that such geometric asperities can attract high stresses due to their discontinuous nature, it becomes clear that their uncertain strain capacity raises safety concerns regarding the proposed strain limits of 3% or 4%. That said, tensile tests on representative specimens containing welds are necessary to quantify the actual strain limit.

In general, experience from previous earthquake events has shown that most steel pipelines exposed to tensile loads performed more than sufficiently, since modern manufacturing techniques are able to satisfy the minimum ductility requirements. When it comes to compressive axial loading, though, emphasis should be placed on the identification of the actual ultimate strain, because the critical shell buckling load has been shown to be highly sensitive to work hardening.

2.4 Flexural failure

Failure due to excessive bending strains of the pipe section is quite rare in steel pipelines because of the high ductility of steel. To this conclusion points evidence from the 1971 San Fernando earthquake event, where a number of buried gas and liquid fuel pipelines were found to have endured approximately 2.5 m of transverse soil dislocation [39]. However, large bending deformations may drive the moment-curvature equilibrium to an ovalization limit or an instability limit, depending on the *R/t* ratio of the pipe.

2.5 Section ovalization

Another possible failure state associated with large radial displacements is the cross-sectional ovalization, also known as the Brazier effect, after the researcher who first derived an analytical ovalization limit for an elastic pipe [40]. Severe bending forces the circular cross-section of the pipe to flatten into an oval-like shape, an effect that accelerates the loss of bending stiffness, differentiating the behaviour as this is predicted by the classical beam bending theory. This does not entail an ultimate limit state, but can pose a serviceability threat to the pipeline carrying capacity. An ovalization limit state developed by Gresnigt [41] is described by the critical change in pipe diameter over the original diameter (also known as the flattening factor):

$$\frac{\Delta D_{cr}}{D} = 0.15 \tag{4}$$

It is important to emphasize that a different approach is needed to establish failure criteria for continuous pipelines with slip, riveted or gas-welded joints. As opposed to pipelines assembled with butt joints, for which failure criteria are mostly functions of pipe performance indicators, in this case failure criteria must be formulated based on joint characteristics. The reason is because this type of joints is generally weaker than the main pipe body. A number of studies involved the estimation of the strength of slip joints with inner [42,43] and outer weld [44], in terms of joint efficiency, namely the ratio of joint to pipe strength. Joint efficiency values lower than 0.40 were obtained in all cases. Damage evidence at gas-welded joints is available from the 1971 San Fernando earthquake, where most of the failures were related to low-quality welding.

2.6 Remarks

It can be argued that some of the existing limit state criteria for buried steel NG pipelines under TGD effects are not well-established. The first reason is that potentially critical conditions controlling the occurrence of the damage modes are ignored from analytical considerations due to the associated analysis complexity. Such are, for instance, the uneven soil resistance around the pipe circumference, the variability of soil properties along the pipeline and the nonlinear pipe-soil contact behaviour, conditions that might be unfavourable (and not extreme cases) to the pipeline seismic performance with regard to shell-type buckling and are not captured by current criteria. Other potentially important aspects that have not received enough attention is the bending-induced shell buckling and the interaction between different modes (e.g., shell- and beam-type buckling).

The second is that the overall approach to the problem lacks robust verification by experimental data. Previous experiments have mostly focused on the derivation of equivalent soil spring constants for analysis purposes, as discussed in Section 3.1.2. Dynamic or pseudo-static physical testing of representative pipe specimens, including the surrounding soil, under controlled laboratory conditions will be valuable in identifying reliably all the variables describing the damage mechanisms, and also in clarifying the conditions under which interaction of different modes can arise. Moreover, based on [26], it can be deduced that beam-mode buckling is more likely to affect smaller-diameter distribution pipelines rather than large-diameter transmission ones. Given the currently available computational demand but also the experimental capabilities, reliable quantification of NG pipeline limit states is deemed of major importance to reduce the associated epistemic uncertainty.

3 ELEMENTS OF PIPELINE SEISMIC RESPONSE ANALYSIS

The crucial factor that differentiates the seismic behavior of buried structures like pipelines from that of aboveground structures is the restraint provided by the surrounding soil and the anticipated dynamic interaction. In contrast to the well-understood, inertia-governed dynamic response of aboveground structures to strong ground motion, subsurface pipelines are minimally affected by seismic inertia forces, because these are of small magnitude as a result of the relatively small pipe mass and are anyway resisted directly by the surrounding soil body. This observation, recognized early by researchers and reflected in design codes [19,38,45–47], further implies that inertial soil-structure interaction (SSI) effects, in the form they manifest in overground structures, are practically insignificant. It follows that the fully dynamic problem can be approximated satisfactorily as a quasi-static one, provided that all important sources of energy dissipation are accounted for. In this respect, it can be argued that the problem of a buried pipeline under TGD is quite similar in terms of mechanics to the problem of a buried pipeline under PGD.

The governing deformation modes are pure axial tension or compression, bending in the vertical or horizontal plane, or combination of these, depending on dominant type of seismic waves (S-waves, P-waves or surface waves), the pipeline alignment with respect to the ray path and the incidence angle of the wave front. A purely axial state of stress, associated with near-uniform normal axial stresses over the pipe section, is produced by shear stress transfer from the soil and can lead to axial buckling or tensile rupture. A flexural state of stress, associated with curvature of the cross-section, is produced by the direct imposition of the soil curvature on the pipe in contact and can result in bending buckling, section ovalization or flexural failure. However, axial seismic demand is deemed more critical as it has been found in several studies that axial strains generally tend to be larger than bending strains (e.g. [6,48,49]), except in the case of pipe bents where the reverse holds [50].

3.1 Soil-pipe interaction

When an earthquake strikes and travelling stress waves arrive at points along a pipeline, it is usually the relative motion between the affected pipe segment and the soil that generates stress in the pipe. We can describe this kind of load as ‘displacement-controlled’, as the pipeline is deformed by the imposed ground motion rather than by seismic inertial forces. For this reason, traditional force-based design is not effective for buried pipelines, rather it is necessary to ensure that ductility levels suffice in this instance (note here that this is underpinned by the fact that pipelines made of cast iron, a non-ductile material, have suffered more extensive damage compared to steel pipelines in past earthquakes). However, the occurrence of relative soil-pipe movement is not a unique condition for pipeline deformation to occur. A pipeline embedded in soil strata having stiffness that varies along its axis is also expected to deform under seismic wave activity due to the different vibrational characteristics of the said strata, even if the pipeline fully conforms to the ground motion (i.e., by assuming zero relative displacements). This case of spatially variable ground motion is of major interest and is more thoroughly discussed in Section 3.2.

As already mentioned, inertial interaction between an NG pipeline and the soil can be ignored in most cases. If, for the case of uniform soil conditions, one further shows that kinematic interaction effects can also be ignored, as demonstrated in Papadopoulos *et al.* [51], the entire soil-pipe interaction (SPI) problem degenerates into a local contact problem driven by the soil motion and can be modelled either rigorously with explicit FE contact formulations or more approximately with equivalent soil springs as discussed below.

3.1.1 Models neglecting soil-pipe interaction

A quite common yet seemingly sound assumption adopted both in design practice and research (e.g. [52–54]) is that the supporting soil possesses considerably greater stiffness than the pipe itself, hence the latter is actually forced to perfectly conform to soil movement; this has also been confirmed by some field tests [6]. From this assumption, it follows that pipe strains and curvatures match the ones developed in the near-field soil. This approach appears conservative, because it leads to higher design strains compared to the case that the pipe is able, to some extent, to resist soil distortion [55].

Along this line of thought, fundamental was the early approach proposed by Newmark [52]. Assuming ground shaking is triggered by a constant plane wave train propagating with velocity c parallel to the pipeline in an infinite, homogeneous, isotropic, elastic medium, he formulated the following simplified yet practical analytical expressions for the axial strain (in case the ground motion is parallel to the propagation direction) and curvature (in case the ground motion is perpendicular to the propagation direction) of a straight pipeline:

$$\frac{\partial u}{\partial x} = \frac{1}{c}\frac{\partial u}{\partial t} \tag{5}$$

$$\frac{\partial^2 v}{\partial y^2} = \frac{1}{c^2}\frac{\partial^2 v}{\partial t^2} \tag{6}$$

where $\partial u/\partial x$ and $\partial^2 v/\partial y^2$ represent the free-field and, by assumption, pipe axial strain and curvature, respectively. Eqs. (5) and (6) can be manipulated to reflect deformation in a buried pipe struck by *P*-, *S*- or *R*-waves under any incidence angle. Kuesel [53] implemented this approach for the earthquake-resistant design of the San Francisco Trans-Bay Tube. Parmelle and Ludtke [56] also conclude that the effect of SPI is negligible. However, Newmark's approach yields credible results mostly for highly flexible pipes, that means pipes with high *R/t* ratios. Typical NG transmission pipelines often have stiffness that may prevent them from fully conforming to soil motion. Consequently, applying Newmark's approach in this case would lead to strain overestimation.

3.1.2 Models considering soil-pipe interaction

When pipeline stiffness is appreciable compared to soil stiffness, as in soft soils or pipelines with relatively low *R/t* ratios, pipeline movement can deviate from that of the soil and SPI effects are likely to play a role in the pipeline response. The simplest and most popular model able to capture this effect is the beam-on-nonlinear-Winkler-foundation (BNWF). In this case, the pipeline is represented by elastic beam elements, while discrete equivalent translational springs of appropriate stiffness are assigned at points along its axis in three orthogonal directions to represent the soil resistance. In a one-dimensional treatment of the general 3D problem in the time domain, the governing equations of motion of a pipeline subject independently to an imposed ground displacement history $w_g(t)$ in the transverse horizontal and $u_g(t)$ in the axial direction are given by:

$$m\frac{\partial^2 w}{\partial t^2}+c_h\frac{\partial w_r}{\partial t}+k_h w_r+EI\frac{\partial^4 w}{\partial x^4}=0 \tag{7}$$

$$m\frac{\partial^2 u}{\partial t^2}+c_a\frac{\partial u_r}{\partial t}+k_a u_r-EA\frac{\partial^2 u}{\partial x^2}=0 \tag{8}$$

where w and u represent the time-dependent pipe displacement components in the transverse and axial direction respectively, $w_r=w-w_g$ and $u_r=u-u_g$, m is the pipe-distributed mass, *EI* and *EA* are the flexural and axial rigidities of the pipe cross-section, and c_h, c_a and k_h, k_a are the equivalent dashpot and spring constants per unit pipeline length in the transverse horizontal and axial directions. If the dynamic terms are ignored, the response is of quasi-static type and Eq. (7) becomes:

$$EI\frac{\partial^4 w}{\partial x^4}=k_h\left(w_g-w\right) \tag{9}$$

Similarly, the quasi-static response in the axial direction is described by

$$EA\frac{\partial^2 u}{\partial x^2}=k_a\left(u-u_g\right) \tag{10}$$

Several soil spring models are available in the literature, and various studies have considered the SPI effect. In an early study, St. John and Zahrah [55] derived a reduction factor to estimate the internal forces of an SPI system from that of a corresponding interaction-free system, making simplifying assumptions about the nature of the oncoming seismic waves. The interpretation of this reduction factor is that consideration of the SPI effects has a favourable effect on the pipe forces. This conclusion is further supported by another study by Hindy and Novak [48]. In this case, a lumped mass beam-model for the pipe was adopted and analysed considering dynamic SPI, in correspondence with the continuous version of the problem described by Eqs. (7) and (8). Two different soil configurations were examined; in the case of a homogeneous medium, it was found that SPI leads to decreased pipe stresses as compared to the ones obtained neglecting it. On the contrary, for a soil consisting of two different layers separated by a vertical plane, stress concentration was evident, this time located close to the vertical boundary, while the pertinent peak values were found higher than the ones predicted without SPI.

One of the first known experimental tests to investigate SPI effects was conducted by Audibert and Nyman [57], who explored the lateral (horizontal) response of steel pipelines buried in sand under a wide range of burial depth-to-pipe diameter ratios. They developed a rectangular hyberbola to represent the soil resistance as a function of the relative lateral movement and then calculated the ultimate soil resistance as a function of the lateral pipe motion:

$$F_{U,lateral} = \gamma' DHN_q \tag{11}$$

where γ' is the effective unit weight of the soil, D is the outside pipe diameter, H is the depth to the pipe centreline and N_q is the bearing capacity factor, estimated from appropriate charts. Hindy and Novak [48] derived analytically linear soil spring constants and dashpot coefficients in the axial and transverse pipeline direction by combining the complex solution of the dynamic plane strain problem of in-phase pipe harmonic vibration and the static solution of Mindlin's problem. The expressions are not included here due to their complexity. O'Rourke and Wang [58] proposed that the axial soil stiffness be twice the effective soil shear modulus.

Later, Nyman [59] investigated the restraints applied on a pipe by cohesionless soil due to oblique vertical-horizontal pipe motion. He proposed an expression for the ultimate soil restraint against the oblique pipe motion as the product of the ultimate soil restraint against vertical pipe motion $F_{\mathrm{U,vertical}}$ and an inclination factor R_i :

$$F_{U,oblique} = R_i F_{U,vertical} \tag{12}$$

with $$R_i = 1 + \frac{0.25a}{90^\circ - 0.75a}\left(\frac{F_{U,lateral}}{F_{U,vertical}} - 1\right) \tag{13}$$

where a is defined as the inclination angle in degrees between the oblique and the vertical soil restraint and $F_{\mathrm{U,lateral}}$ can be evaluated from (11) or other sources. To completely describe the nonlinear force-displacement relationship, Nyman recommends the following values for the yield displacement soil required to mobilize the oblique ultimate soil restraint:

$$\delta_{y,oblique} = \begin{cases} 0.015H & \text{for dense geomaterials} \\ 0.025H & \text{for loose geomaterials} \end{cases} \tag{14}$$

To validate the available analytical models against experimental data, Trautmann and O' Rourke [60] performed a series of multi-parametric lateral loading tests to assess the response of subsurface, typically-sized pipelines to lateral soil motion. A hyperbolic function was derived to represent the average lateral force-displacement curve of the obtained test data, expressed in dimensionless form as:

$$F/F_U = \frac{\delta/\delta_y}{0.17 + 0.83\delta/\delta_y} \tag{15}$$

where $F_U = \gamma HDLN_h$ is the ultimate soil force, with L and N_h standing for the length and the horizontal force factor, respectively. Appropriate values for the latter parameter may be sought in relevant charts as a function of depth-to-diameter ratio and friction angle. Test results also indicated a strong variation of the yield displacement δ_y of the soil with the soil density, ranging from $0.13H$ for loose soil, $0.08H$ for medium soil and $0.03H$ for dense soil.

Selvadurai [61] gave the vertical elastic stiffness of a buried pipeline under ground movement as $K_v = 1.3G/(1-\nu)$. In order to characterize the transverse horizontal and axial SPI described by Eqs. (9) and (10), St. John and Zahrah [55] used a foundation modulus obtained by manipulating the solution to the Kelvin's problem of a static point load applied within an infinite, homogeneous, elastic, isotropic medium. The result was expressed as:

$$k_a = \frac{16\pi}{\ell}\frac{(1-\nu)}{(3-4\nu)}GD \tag{16}$$

where ν, G are the Poisson's ratio and shear modulus of the medium and D the outer pipe diameter. In the same manner, but utilizing the solution to the Flamant's problem, they arrived at an estimate for the foundation modulus that governs the pipe response to transverse vertical soil motion:

$$k_v = \frac{2\pi G}{(1-\nu)}\frac{D}{\ell} \tag{17}$$

Concerned with the evaluation of axial soil springs, El Hmadi and O' Rourke [62] aimed to verify the theoretical and empirical predictions for the axial spring stiffness available at that time, taking advantage of the experimental data provided by a previous full-scale field test [63]. After performing a back-calculation on the governing displacement functions and considering the strain-dependent nature of the soil shear modulus, they ended up with an upper and lower bound value for the axial spring constant k_a as a function of the soil shear modulus G:

$$1.57G \leq k_a \leq 1.70G \tag{18}$$

This range of values apparently lies within and consequently partly confirms the wider range provided by the then existing literature $G \leq k_a \leq 3G$. Another important finding of this study is that the inertial axial force induced in the pipeline during the test was over two orders of magnitude *lower* than the soil restraint developed, thus confirming that pipeline inertia is insignificant. O' Rourke and El Hmadi [47] calculated the peak frictional resistance per unit length that develops at the soil-pipe interface under relative axial motion as the product of the mean applied normal force and the coefficient of friction:

$$F_{U,axial} = \mu\gamma' H\left(\frac{1+k_0}{2}\right)\pi D \tag{19}$$

where μ represents the coefficient of friction, k_o is the coefficient of lateral earth pressure and πD the circumference of the pipe. Matsubara and Hoshiya [64] derived the axial elastic stiffeness using the elasticity theory as $K_\alpha = 2\pi G/(\log\lambda)$, where λ is defined as the ratio of an imaginary outer radius at which displacements vanish and the pipeline radius.

In another experimental effort, Hsu *et al.* [65] dealt with the response of pipes buried in loose sand and subjected to oblique-horizontal increasing displacement. Specifically, a large-scale test was carried out involving various pipe specimens and depth configuration, wherein the pipe was successively placed at horizontal orientations in different, gradually increasing inclination angles with respect to the direction of movement. The goal was to evaluate the longitudinal and transverse horizontal (lateral) soil restraint components for each test setup of the oblique pipe. Their results

Table 1. Soil-pipe interaction models proposed in the literature, described by either the ultimate soil restraint or equivalent spring constants (all parameters and variables involved are explained in the body).

Reference	Relationship	Applicability
Audibert and Nyman (1977)	$F_{U,lateral} = \gamma' DHN_q$	Lateral direction; steel pipe in sand
O'Rourke and Wang (1978)	$k_a = 2G$	Axial direction
Nyman (1984)	$F_{U,oblique} = R_i F_{U,vertical}$	Oblique direction in cohesionless soil
Trautmann and O' Rourke (1985)	$F/F_U = \dfrac{\delta/\delta_y}{0.17+0.83\,\delta/\delta_y}$	Lateral direction; δ_y ranges from $0.03H$ to $0.13H$ depending on soil density
Selvadurai (1985)	$k_v = 1.3G/(1-\nu)$	Vertical direction
St. John and Zahrah (1987)	$k_a = \dfrac{16\pi}{\ell}\dfrac{(1-\nu)}{(3-4\nu)}GD$	Axial direction; elastic stiffness
El Hmadi and O' Rourke (1988)	$1.57G \le k_a \le 1.70G$	Axial direction
O' Rourke and El Hmadi (1988)	$F_{U,axial} = \mu\gamma' H\left(\dfrac{1+k_0}{2}\right)\pi D$	Axial direction; sand backfill
Matsubara and Hoshiya (2000)	$k_\alpha = 2\pi G/(\log\lambda)$	Axial direction; infinite homogeneous soil
Hsu *et al.* (2001)	$\begin{cases} F_{axial-oblique} = F_{axial}\cos a \\ F_{lateral-oblique} = F_{lateral}\sin a \end{cases}$	Lateral direction in loose sand

indicated that the axial-oblique restraint can be determined simply by multiplying the axial force of the corresponding purely axial pipe ($a = 0^\circ$) with the cosine of the inclination angle, while to obtain the lateral-oblique restraint, a multiplication between the lateral force of the associated purely lateral pipe and the sine of the inclination angle is sufficient:

$$F_{axial-oblique} = F_{axial}\cos a \tag{20}$$

$$F_{lateral-oblique} = F_{lateral}\sin a \tag{21}$$

where a is the inclination angle between the orientation of the pipeline and the direction of movement. Table 1 summarizes all SPI spring models presented in this section.

The American Lifeline Alliance presented a report [66] that contains mathematical expressions describing the constitutive behaviour of nonlinear lumped soil springs in each of four principal

Table 2. Ultimate soil force and relative displacement relationships for soil-pipe relative motion proposed by the ALA [66].

Spring direction	Ultimate soil restraint	Ultimate relative displacement
Axial	$\pi Dac + \mu\gamma' H\left(\frac{1+k_0}{2}\right)\pi D$	$3 \sim 10\,\text{mm}$
Lateral	$cDN_{ch} + \gamma' DHN_{qh}$	$0.04(H + D/2) \le 0.10D \sim 0.15D$
Vertical uplift	$cDN_{cv} + \gamma' DHN_{qv}$	$\begin{cases} 0.01H \sim 0.02H < 0.1D & \text{dense to loose sands} \\ 0.1H \sim 0.2H < 0.2D & \text{stiff to soft clays} \end{cases}$
Vertical bearing	$cDN_c + \gamma' DHN_{qb} + \gamma \frac{D^2}{2} N_\gamma$	$\begin{cases} 0.1D & \text{for granular soils} \\ 0.2D & \text{for cohesive soils} \end{cases}$

a : adhesion factor; c : backfill soil cohesion; N_{ch}, N_{qh}, N_{cv}, N_{qv}, N_{qb}, N_c, N_γ : bearing capacity factors in the horizontal, vertical uplift and vertical bearing direction (subscript c denotes clay, q denotes sand)

directions of pipe motion, i.e. axial, lateral, vertical uplift and vertical bearing. In all cases, the nonlinearity of the soil is idealized as an elastoplastic bilinear curve, hence it is only one point that is actually needed to define each curve. These models provide a way to estimate both the maximum soil restraints and the corresponding relative displacements. The relationships (Table 2), extensively used in design practice, were derived assuming uniform soil conditions and are based on Refs. [67,68].

3.2 Spatially variable seismic demand along the pipeline

Spatial variability in earthquake ground motion (SVEGM) can be interpreted as the differences expected in frequency content, amplitude and phase angle of seismic signals captured at distant stations on a local scale; this observation was consolidated over three decades ago, when researchers [69,70] started analyzing the ample accelerogram data obtained from densely installed strong motion recording arrays, in particular the SMART-1 array in Taiwan. SVEGM is a physical phenomenon of stochastic nature, in the sense that its occurrence can only be predicted with a degree of uncertainty due to the complex, multi-parametric underlying mechanisms that contribute to its generation.

These variations in the seismic ground motion are attributed to three main factors [71]: (a) the transmission of the waves at finite velocity (*wave passage effect*), which intuitively results in different arrival times at different recording stations, (b) the gradual reduction in the coherency of the waves as a result of successive scattering, such as reflections and refractions, that occurs along their path through the inhomogeneous earth strata (*ray-path effect*), and due to the varying superposition of waves originating from different points of an extended seismic source (*extended source effect*), collectively known as the '*incoherence effect'*, (c) the different local soil conditions at remote stations that primarily affect the amplitude and frequency content of the incoming waves (*local site effect*). Additional causes of the phenomenon have also been recognized: the attenuation of seismic waves along their path, resulting from the gradual dissipation of wave energy into the soil medium, and, though not critical in the case of pipelines, the relative flexibility of the soil-foundation system that may ‘filter’ certain frequencies of the incoming wave field [72].

SVEGM and its effects on extended structures such as bridges, dams etc, have been rigorously investigated by modeling the earthquake ground acceleration as a random signal of time using analytical [73], numerical [74], field [75] and experimental [76,77] methods. Descriptors of the probabilistic properties of the ground motions have been established and used to reflect the sources of spatial variability [78]. Random vibration analysis or deterministic time-history analysis using simulated spatially variable ground motions as input are employed to assess the effect of the phenomenon on the response of various structures.

It is understood that SVEGM is very relevant to buried pipeline systems. Given the spatial extent of the structure, the input seismic excitation can always and should be treated as a spatially variable one. Along these lines, SVEGM in buried pipeline problems falls in two major categories: (a) due to the wave passage effect and (b) due to local site effects. The majority of the published research has focused on the first, as will be become obvious in Section 3.3. Local site effects have received less attention comparatively.

Local site effects may result from gradients in soil properties (medium inhomogeneity), features of irregular topography (e.g., hills, ridges, canyons and cut-and-fill slopes) and special subsurface geomorphic conditions, such as a soft surficial sediment sharing an inclined border with stiff rock (valley setting). The presence of any of the above along the route of a buried pipeline, combined with ‘appropriate’ seismic excitation, can profoundly amplify the ground motion, alter its frequency characteristics and spatial profiles, prolong its duration, and induce substantial ground strains and curvatures (e.g., see [79–83]), which in turn can cause pipeline deformation. In Figure 3, some idealized scenarios of such sites and loading conditions are identified and sketched: (a) a site consisting of two horizontally adjacent soil layers of different shear wave velocities and (b) a soft alluvial valley of trapezoidal shape, both excited by vertically propagating *S*-waves of varying polarization. In case (a), *S*-wave polarization in the pipeline direction induces axial strain in the pipeline near the boundary (marked with red), while the generated parasitic vertical motion forces the pipeline to bend in the vertical plane (indicated by a black curve). In this situation, coupled axial-bending shell-buckling and ovalization may appear, while tensile fracture is generally not anticipated. Polarization in the transverse direction induces only bending in the horizontal direction near the boundary which is likely to cause ovalization of the cross section and bending buckling. The stress state is similar in case (b), with the difference that peak strains and curvatures are located near the valley edges. One immediately realizes that if the wavefield is incident under angle, or the pipeline is placed obliquely with respect to the soil particle motion, multiple motion components will be simultaneously applied on the pipeline.

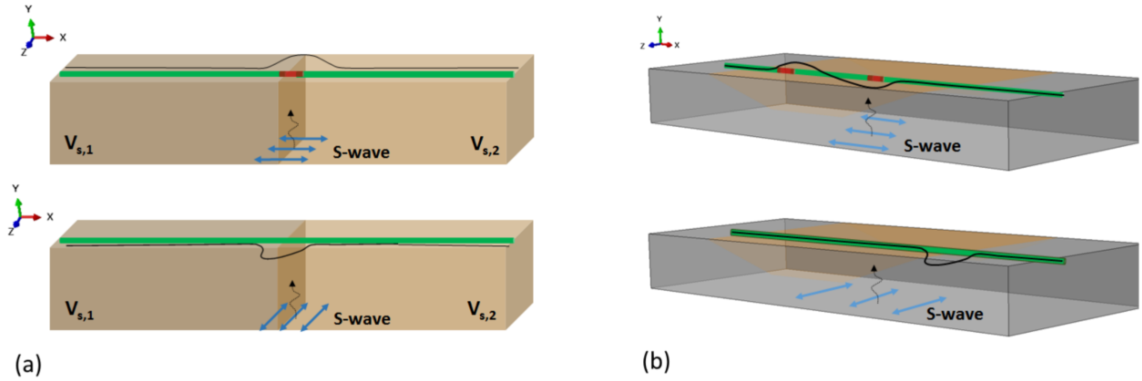

Fig. 3. Buried NG pipeline crossing: (a) two laterally adjacent soil layers of different V_s; (b) a soft alluvial valley setting.

The effect of inhomogeneous soil on pipeline seismic demand was first studied by Hindy and Novak [48] using dynamic equilibrium of an elastic lumped-mass beam model of the pipeline and appropriate soil springs and dashpots. A major conclusion was that body waves travelling along a pipeline laid through two different soils cause peak axial and bending stresses near the boundary of the two media, and are larger than the ones in the homogeneous case. Several of the earliest contributions on the effect of SVEGM on the response of buried pipelines are attributed to Japanese researchers. Nishio *et al.* [84,85] conducted laboratory tests of buried pipelines in valley and cut-and-fill settings subject to horizontal base excitation. Analytical methods have also been used to study the strain response of buried pipelines laid through dipping soil layers [86], cut-and-fill embankments [87], riverbeds [88] and multiple soil media [89].

Buried pipelines under incoherent ground motion have also been the subject of scrutiny. Zerva *et al.* [90] and Zerva [72] examined in the stochastic domain the axial and transverse response of segmented and continuous pipelines to differential ground motion. Random vibration analysis of analytical pipeline models was carried out using as input the stochastic properties of ground motions recorded at the SMART-1 array. By comparing results for partially and perfectly coherent motions, a close match was found between displacements of continuous pipelines, a circumstantial finding attributed to the fact that the same rigid body mode was excited in both cases. However, partially correlated motions gave higher stress values. Further, it was observed that axial stresses become dominant as the slenderness of the continuous pipeline increases, while bending stresses become sizable when the pipe diameter is large. The results of another effort [49] revealed that axial strains are the principal source of deformation over bending strains in continuous, large-diameter pipelines (Figure 4). It was also shown that the selection of the incoherence parameter on the pipeline response is critical (Figure 5). Upon inspection of the figures, it can be seen that the maximum axial strains are at least two orders of magnitude lower than the steel elastic limit and the commonly used limit state strains.

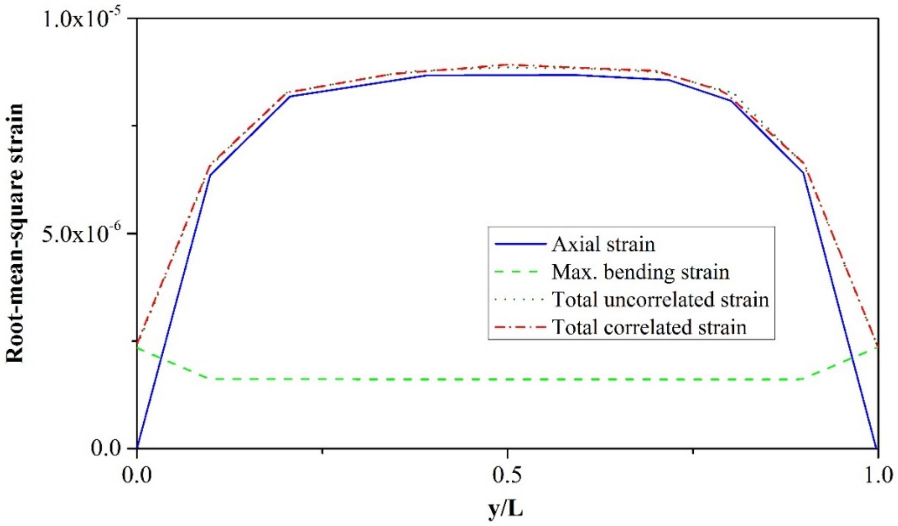

Fig. 4. Distribution of root-mean-square strains along the pipeline longitudinal axis *y* for pipe orientation that coincides with the epicentral direction of the input motion, as calculated by Zerva (1993) (adapted from [49]).

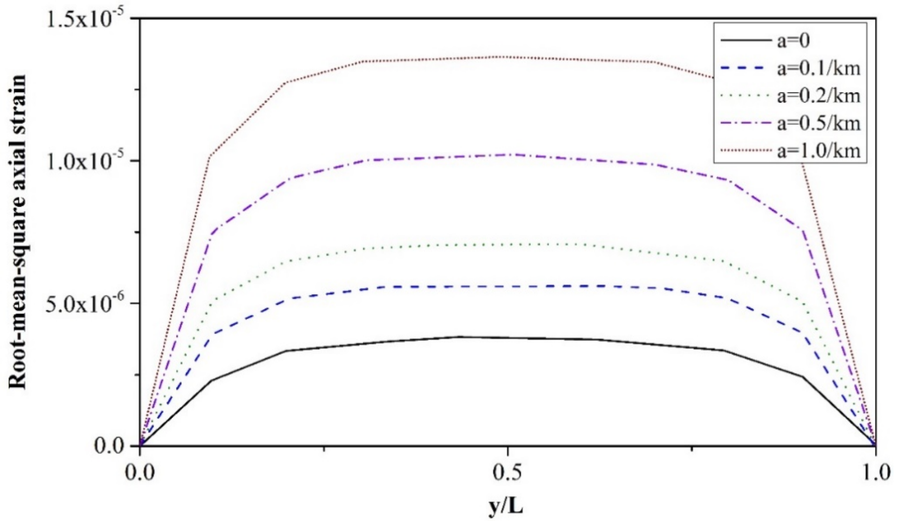

Fig. 5. Distribution of root-mean-square axial strains along the pipeline longitudinal axis *y* for different values of the incoherence parameter, as calculated by Zerva (1993) (adapted from [49]).

Zerva [91] further dealt with the effect of differential ground motions on the response of various lifeline structures, including underground pipelines. Two coherency decay models [92][93] were used and it was found that pipeline axial strains are maximized when the motions are totally incoherent, i.e. the differential displacements at the input stations are maximum. Specifically, for the second coherency model, an increasing trend was observed for the seismic strains with stronger decay (denoting increasing incoherence). More recently, Lee *et al*. [94] applied multiple seismic excitation on a BNWF model of a pipeline in a 3D nonlinear time-history analysis, showing that the pipeline displays varying distribution of the axial relative displacement along its length, with peaks appearing in the region of differing imposed excitations. For the bending response, calculated pipeline demand for a specific input ground motion reached half the respective capacity.

At the time of writing, the authors of this were expending efforts to investigate numerically the impact of non-uniform site conditions on the stability of high-pressure steel natural gas pipelines. To this end, the buckling capacity of the pipeline is evaluated in view of the demand imposed by the vibrating soil. The originally complex problem is split in two stages: (a) determination of the time-varying site response at the pipeline depth and subsequently (b) application of the critical response profile as a spatially variable displacement demand on the pipeline. The latter issue is described better in Section 3.3. In terms of site response, the scenarios illustrated in Figure 3 are considered. Parametric 2D plane-strain viscoelastic and equivalent-linear site response analyses are conducted with Ricker-type wavelets and real ground motion records as input to detect the most critical TGD cases. Some sample results are shown in Figures 6 and 7. Figure 6 shows contours of the axial strain synthetics at the ground surface for equivalent-linear soil response of the sites displayed in Figure 3 under high-intensity Ricker pulses. It is clear that peaks appear near the material discontinuity with magnitudes of one order higher (~ 2%) than the elastic ones, a result with potential implications on the pipeline demand. In Figure 7, the critical horizontal displacement profiles derived based on the maximum compressive strain are plotted for different input excitations, revealing that the maximum differential displacement load on the pipeline shows strong dependence on the exciting frequency.

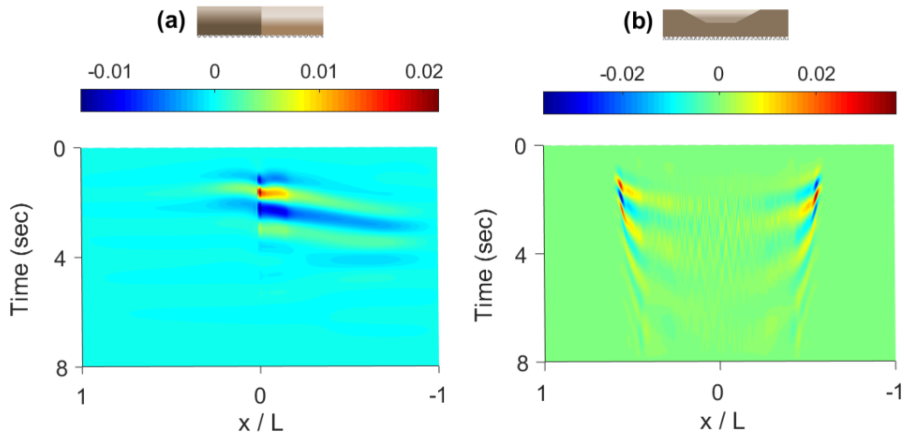

Fig. 6. Time-variation of axial strain field at the surface of the equivalent-linear sites of Fig. 3 for vertically incident acceleration Ricker pulse with 0.5 Hz and PGA=0.2g (*L*= half-length of the domains)

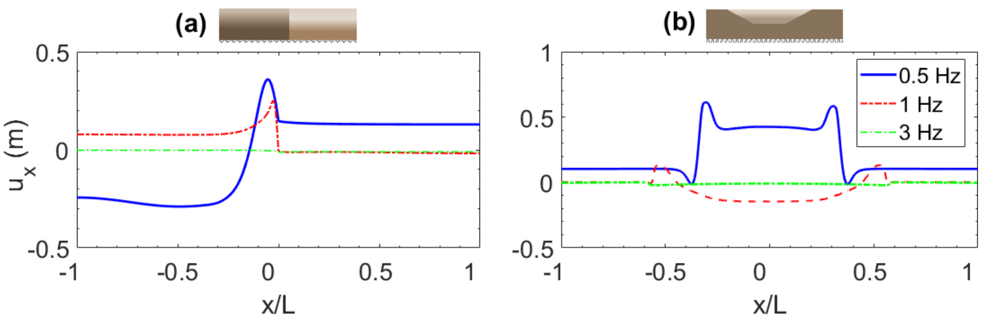

Fig. 7. Critical horizontal displacement profiles at the surface of the equivalent-linear sites shown in Fig. 3 for vertically incident acceleration Ricker pulses with PGA=0.2g and varying frequency.

3.3 Analysis methodologies employed in literature

The choice of a suitable methodology to estimate the pipeline response to strong ground shaking is case-specific and largely depends on the response quantity and damage mechanism of interest, as well as the desired degree of accuracy. In general, the physical problem in its entirety is extremely complex and uncertain, as it involves wave propagation in elastic/inelastic semi-infinite soil media, inherently random time-varying input excitation, nonlinear surface contact between the pipeline and soil, shell pipe mechanics, potential geometric nonlinearities, very large dimensions, nonhomogeneous site with uncertain dynamic properties, potential geometry defects and material inelasticity of the pipeline, and time-dependent response. All these complexities render a fully 3D numerical approach not only computationally prohibitive, but also unjustified in view of the involved uncertainties; hence, reliable simplification of the problem is essential.

Typically, simplification steps are taken with regard to two constituents of the physical problem: (a) modelling of the pipeline behaviour and (b) modelling of the supporting soil and/or soil-pipe contact conditions (SPI). As regards item (a), if one wants to obtain simply a rough estimate of the pipeline seismic demand (axial or bending) and compare it with the respective capacity, they commonly resort to the classical beam theory. In this manner, axial and bending deformations are assumed uncoupled, while the hoop stress component, which might become important, cannot be captured. The ability to capture shell buckling modes and section ovalization is also precluded.

On the other hand, if the goal is to check for the possibility of shell bifurcation or cross-section ovalization, or account for hoop stresses due to pressurization and gravity, use of one of the available shell theories is inevitable in order to accurately describe the cross-sectional deformation and the distributions of membrane and bending strains. Hybrid approaches have also been reported (e.g.,[95]), wherein the critical pipeline segment is modelled as a cylindrical shell and the remaining segments as beams.

As for item (b), the simplest method is to neglect any relative motion between pipe and soil, as long as this can be warranted by the problem characteristics; in this way, the assumed input excitation can be directly applied on the pipeline and a purely structural analysis of a 2D or 3D pipeline model can be performed. A method of better accuracy is the use of equivalent nonlinear soil springs to account for soil resistance in the tangential and normal directions, as already presented in Section 3.1.2. In both these methods, soil response is assumed as uncoupled and its explicit dynamic simulation is excluded from the analysis; instead, the input excitation is taken directly from recorded outcrop ground motions at different stations or is calculated as a function of the incidence angle for seismic waves of idealized, typically sinusoidal, shape. The use of general 3D elasticity theory to represent soil behavior is very rare, and so is site response analysis to propagate the oncoming wavefield from the far-field to surface. All combinations between variants of items (a) and (b) have been reported in the literature as discussed below.

Sakurai and Takanashi [6] were among the first to study the dynamic stresses on a buried pipeline by conducting field experiments during the Matsushiro earthquake sequence. They observed that axial pipe deformations match the ground ones when the earthquake intensity is mild enough to not induce slip, and this was confirmed by the solution they derived for Eq. (8) (ignoring the damping term). Shinozuka and Koike [96] extended the results of [6] to calculate conversion factors between the induced soil and (straight and bent) pipe axial strains in a homogeneous medium due to a P- or R-wave propagating parallel to the pipeline, taking into account the possibility of slippage (nonlinear axial interaction). Comparison between the dynamic and the quasi-static conversion factors revealed a minor effect of pipeline inertia. From the perspective of structural stability, Lee *et al.* [25] used an elastic-plastic cylindrical shell formulation for a buried pressurized pipeline in a homogeneous elastic medium, based on the simple flow plasticity theory and a variational formulation for the equations of motion, to check for the stability of the dynamic equilibrium of the pipe shell. In their treatment, they ignored SPI in the axial direction and assumed a lateral soil restraint in the form of distributed elastic radial springs. Their solutions showed that the critical axisymmetric buckling stress and strain of the pipeline under dynamic conditions are essentially the same as under static conditions. In another seminal work, Wong *et al.* [97,98] considered in its three dimensions the problem of a long pipeline shell buried in an elastic homogeneous halfspace under obliquely incident body or surface waves. They arrived at an analytical solution of the equations of elastodynamics describing the coupled motion of pipeline and soil by using eigenfunction expansions of the wave potentials. In this way, they accounted for inertial and kinematic SPI, as well as scattering of the waves by the free surface. O'Rourke and El Hmadi [47] studied the axial behavior of a continuous elastic pipeline embedded in a homogeneous elastic soil under Rayleigh wave propagation in the pipeline direction (Eq. (8)). Elastic-perfectly plastic frictional behaviour at the soil-pipe interface was considered through Eq. (19). They also proposed a design methodology based on the correlation between ground axial strain and interface frictional strain. Application of this on a typical buried steel pipeline case showed that the axial pipe strain produced by an R-wave of PGA=0.35g reached 35% of the yield strain. Yun and Kyriakides [26] examined in detail the conditions under which a buried pipeline loaded in compression may bifurcate plastically into a beam- or an axisymmetric shell-mode, as well as the potential of interaction between the two. To formulate the problems analytically, they used large-deflection beam kinematics for the first and Sander's nonlinear thin shell theory for the second mode, respectively, coupled with incremental plasticity laws and initial geometric imperfections. SPI was assumed as in [25] but through a nonlinear model calculated by solving the problem of a circular soil cavity expanding uniformly.

In more recent works, Kouretzis *et al.* [99] deployed elastic shell equations to analyze the distributions of axial and hoop strains of a long cylindrical structures in uniform elastic soil or soil-over-bedrock due to out-of-phase vibration induced by travelling harmonic S-waves, incident under angle. Optimization of the closed-form solutions with respect to the angle variables involved led to critical strain expressions for seismic design. Hatzigeorgiou and Beskos [100] developed the finite element code SINUS to analyze directly seismic SSI effects in 3D rock-tunnel systems, considering the inelastic behaviour of both materials through the continuum theory of elastic damage. Their results showed the reliability and efficiency of the methodology adopted, and also that SSI effects are negligible for tunnels in soft rock. Focusing on steel pipe bends, Saberi *et al.* [101] used a hybrid 3D shell-beam pipeline model where the bend part is represented by shell elements and the straight parts by beam elements. SPI was taken into account using the ALA spring models for uniform soil, while nonlinear pipe end springs were used to represent pipe continuity. Nonlinear response history analyses were performed in all three principal directions using real ground motions having phase difference. Nourzadeh and Takada [102] use the BNWF model combined with the ALA soil springs in their numerical parametric investigation of the response of buried steel NG distribution pipelines to input earthquake ground motion in three directions. Analyses postulate that pipelines experienced local buckling for PGAs greater than 0.6g; however, performance criteria are too loosely defined to allow safe judgment based on this observation, since a shell analysis was not performed. Papadopoulos *et al.* [51] employed a two-step numerical methodology to shed light into the effects of SVEGM on the demand of a buried pipeline longitudinally crossing a basin section: they first performed 2D viscoelastic site response analysis under in-plane S-wave propagation to determine the soil response histories at the pipeline depth, and then applied these 2D excitations on a separate BNWF pipeline model to perform a 3D nonlinear time-history analysis (Figure 8).

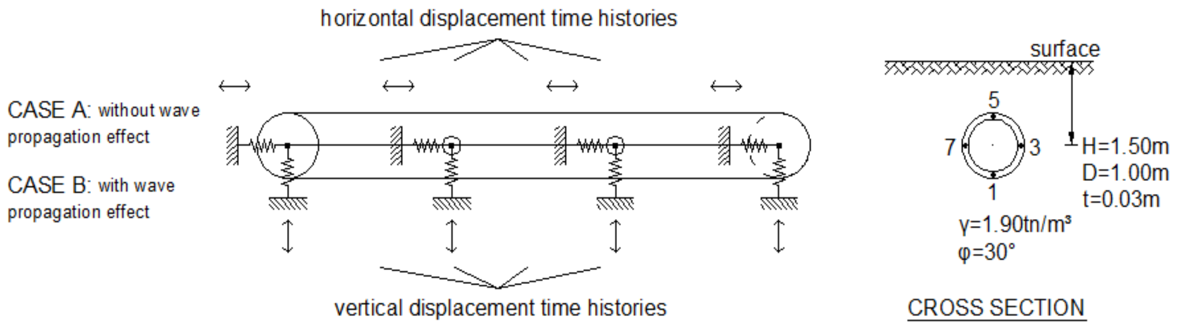

Fig. 8. BNWF model of a pipeline used in Ref. [51], with equivalent soil spring support in two directions.

Following the latest trend in research necessitating the use of sophisticated numerical simulations to capture the nonlinear behaviour and bifurcation of shell-type structures, several studies have explored the response of buried steel pipelines under PGD effects. In a series of publications [23,103,104], Vazouras and his co-workers used 3D shell and solid finite elements (FE) for the soil-pipe model to analyze the static axial and bending strains in buried steel pipelines crossing active strike-slip faults under angle, also considering the influence of pipe continuity by deriving nonlinear springs for the pipe ends. SPI was represented rigorously by the use of contact elements at the interface. Daiyan *et al.* [105] developed a similar 3D FE model to validate centrifuge tests; their findings indicate that SPI can exhibit strong coupling for oblique loading. In the same fashion, Sarvanis *et al.* [106] enhanced this approach by calibrating model parameters through full-scale tests. Vazouras and Karamanos [107] extended the previous models to study the mechanical performance of pipe bends; their results substantiated their increased flexibility. Chaloulos *et al.* [108,109] and Kouretzis *et al.* [110] employed 2D plane-strain soil-pipe FE models with interface contact elements to study the trench effects on the soil-pipe response subject to PGD. In analytical treatments of pipelines under PGD problems, Karamitros *et al.* [95], adopted a BNWF model and a secant modulus solution method to develop a design methodology to estimate inelastic pipeline axial and bending strains generated by strike-slip fault movement, while Trifonov and Cherniy [111] contributed a plane-stress plasticity model that accounts for internal pressure, temperature variation and bending stresses, combined with a BNWF pipeline model to effectively predict the inelastic stress and strain distributions over the pipe cross-section due to fault displacements. The last works concerning PGD might seem irrelevant to the topic of this study, but in reality they are not. Given that previous research has shown that dynamic amplification in TGD-governed problems is not important, several of the analysis approaches taken to solve PGD problems can be effectively applied on TGD problems with the appropriate modifications.

As part of the ongoing work briefly mentioned in Section 3.2, the authors of this have undertaken a two-level analysis approach to capture potential buckling phenomena due to SVEGM-induced compressive axial strain and curvature in the pipeline. A long 3D shell finite element model has been encased by a near-field, caisson-type 3D continuum soil model representing the trench. Ignoring classical SSI effects (both kinematic and inertial), the pseudo-static nonlinear response of the pipe-soil model is computed for the critical in-plane soil displacement profiles obtained from 2D plane-strain site-specific response analysis (Figure 9). With this method, the contact state can be evaluated with precision over the entire contact surface: the frictional behaviour is controlled by a Coulomb law, a separation/no-penetration rule is used for the normal behaviour, and also their coupling is guaranteed. The initial stress equilibrium in the domain due to gravity and pipe internal pressure loading is directly computed. For a typical pipeline with R/t=30 and σ_y=450 MPa buried in a site similar to scenario (a) of Figure 3 and subject to the axial ground strains generated by the 1979 Imperial Valley earthquake (*PGA*=0.31g), results reveal that, although sliding initiates after a limit stress and spreads, there is strong interaction between the axial load and bending moment in the vertical plane within a short critical segment near the inhomogeneity feature, which essentially reduces the axial buckling limit load of the pipeline. The evolution of strain localization leading eventually to the development of two nearby lobes is displayed in Figure 10, where different stages are associated with the respective points on the average $\sigma_x - \delta_x / l_{cr}$ and $M - \kappa$ paths.

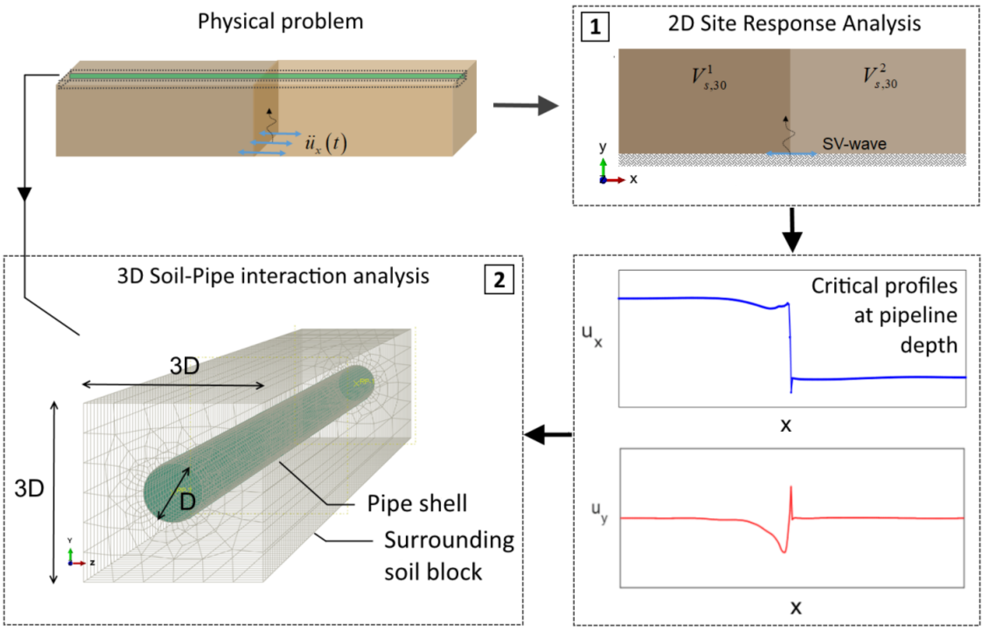

Fig. 9. Illustration of a two-stage methodology to analyze local site effects on the seismic response of a buried pipeline: (1) site-specific seismic response analysis and derivation of the critical motion profiles along the assumed pipeline; (2) aspect of a 3D continuum-shell SPI FE model able to capture local buckling phenomena in the pipeline upon static application of the critical displacement patterns from stage (1).

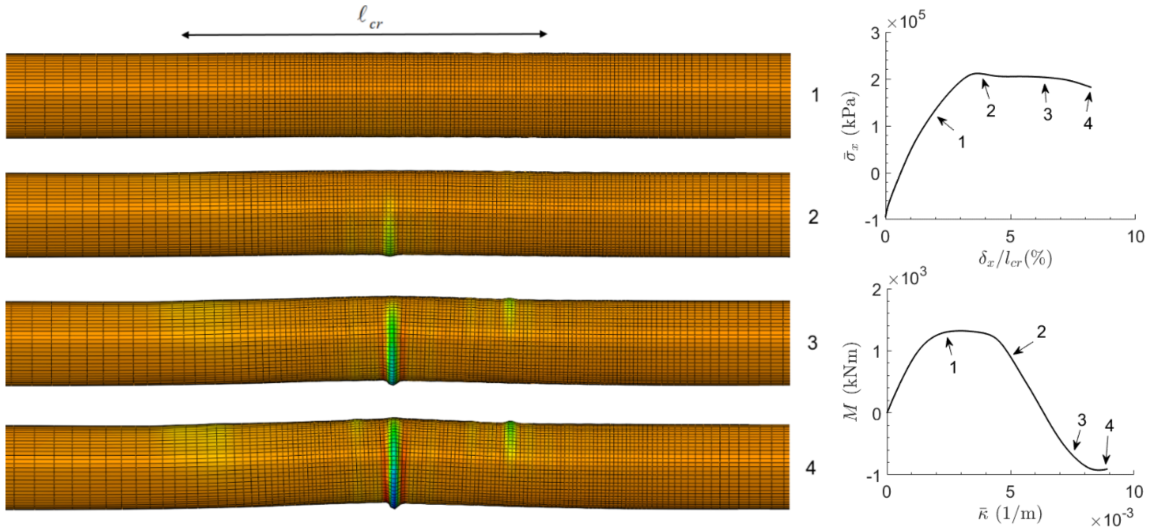

Fig. 10. Left: the successive stages of deformation localization in the pipeline due to axial load-moment interaction, with axial strain contours depicted; right: nominal axial stress-shortening and bending moment-axial curvature plots (control sections are taken to account for the response in the critical zone of the pipeline).

3.4 Implications and recommendations

There are certain key problem parameters that need first to be well understood and defined before we gain confidence in our model predictions.

Geologic and geomorphic conditions

One major consideration is the overall geologic and geomorphic conditions in the region of interest. Crucial to the choice of a suitable analysis methodology is the reliable knowledge of the degree of soil stiffness variation in the direction of pipeline route, but also with depth, particularly if the bedrock is inclined. To this end, in-situ field surveys can contribute useful data on the real soil properties. If the soil domain where the pipeline is supposed to be buried is relatively uniform, then strains can arise only as a result of the apparent propagation velocity of the travelling waves, depending again on the dominant wave type and the incidence angle, or as a result of strong relative soil-pipe motion under a fully coherent wavefront, when the wave amplitude is large. In these cases, it has been shown that the expected pipeline strains are generally orders of magnitude smaller than steel yield limits, hence a highly sophisticated modelling approach to predict the pipeline seismic response is rather unnecessary. If, however, strong soil heterogeneities or special topographic features, such as basins, hill crests and toes and cut-and-fill embankments, are present along the pipeline path, complex scattering of the wavefield can drastically amplify motion, change the frequency content and induce significant displacement gradients. In such cases, more elaborate models of the pipeline and SPI are recommended to predict the biaxial state of stress, particularly if shell-mode buckling needs to be captured. Also, 2D or even 3D site response analysis is deemed appropriate in some instances to evaluate reliably the differential surface free-field motion. The sub-structuring DRM method [112] is another viable option, if one wants to resort to a large-scale simulation containing both the source, path, and local site effects.

Distance to source

A second consideration is the proximity of the location of interest to the earthquake source, which has impact on the prevailing types of seismic waves and their frequency content. A pipeline passing near the source of an earthquake is more likely to be stricken by high-amplitude, high-frequency vertically propagating body waves. It follows that pipeline distress can emerge in this case by in-phase relative movement between the pipeline and the soil, where a 2D dynamic plane-strain model is suitable, or by local site effects. On the other hand, in an apparently more complicated situation, a buried pipeline in sufficient distance from the earthquake source can be affected simultaneously by both nearly-vertically propagating body waves and surface waves of lower frequencies and larger amplitudes. It has been observed that the predominant wavelength of Rayleigh waves is a controlling parameter for the level of stresses developed in a buried pipeline [47] The above remarks have implications on the selection of the input ground motion to be used in a site response or more directly a pipeline response analysis.

Trench soil

The trench soil also deserves special attention. In common pipeline trenching operations, the excavated trench soil is backfilled after the pipeline is laid, and compaction follows. The initial contact state of the soil-pipe system depends on the quality of the backfilling and compaction works. Sometimes, the compaction can increase the lateral earth pressure coefficient up to unity or more; in turn, the frictional resistance, taken from the Coulomb friction law as a function of soil pressures, is raised, and this can consequently favour the development of larger pipe stresses. The tangential interface behaviour is controlled by the coefficient of interface friction, which is usually a linear function of the angle of shearing resistance of the trench soil. Some typical values of the coefficient of interface friction for buried steel pipelines are given in [47], but generally its value is not known with certainty and, even if it was known, it would possibly vary along the pipe length. Notably, the effect of pipeline steel scour on the SPI has also been investigated [113] and it was found that tangential interaction depends on the unsupported length of the pipe due to scour. Further, Chaloulos *et al.* [108,109] and Kouretzis *et al.* [110] explored the effect of a narrow trench on the evolution of the soil failure surface and peak pipeline force under lateral pipeline motion. Using experimentally validated numerical models, they show that the commonly used assumption of an infinitely wide trench can lead to underestimation of the actual response quantities. Moreover, the trench soil properties are a determining factor to the uplift resistance of the pipeline, which is of interest when ground motion with significant vertical components is expected.

Internal pressure

Another key factor specific to NG pipelines is the level of internal pressure. Pipelines belonging to the high-pressure transmission grid develop large initial circumferential tensile stresses (30-40% of the yield stress) as a result of uniform pressurization. This can have mixed effects on the overall seismic performance of the pipeline. In constraint-free circular cylindrical shells under uniform axial compression, the presence of internal pressure lowers the whole inelastic part of the response as a result of the produced state of stress, and this reduction is sharper for higher pressures. It follows that yield, bifurcation and collapse (if occurring in the plastic range) loads are reduced compared to the no-pressure case [114]. If the shell is under axial compression, pressure also stiffens the pre-yield response. In buried pipelines, however, Lee *et al.* [25] report that pressurization has the opposite effect, i.e., it raises the pipe buckling stress. Another intuitive effect of internal pressure is that it tends to smooth out non-axisymmetric imperfections. Despite the aforementioned effects, the seismic performance of a pressurized buried pipeline is not expected to be drastically modified; however, this aspect calls for further scrutiny under simultaneous consideration of the soil restraint.

Pipeline geometric imperfections

Initial pipe wall imperfections are an issue that deserves due consideration. Thin-walled cylindrical shells are known to be highly imperfection-sensitive structures, and this can be manifested by the severe discrepancies in buckling loads between theoretical elastic solutions and experiments with real specimens [115]. This sensitivity is also evident for cylindrical shells of lower *R/t* ratios, where buckling is expected in the inelastic range. Pipelines may suffer from two different types of geometric imperfections: 'load' imperfections caused in-situ by the depth-dependent soil pressures towards the pipeline walls, and pre-existing geometry imperfections resulted from such operations as manufacturing process (residual stresses), transportation, girth welding and laying, all of which can cause deviations from the perfect geometry. For instance, ArcelorMittal states in its API-5L X65 line pipe stock specifications [116] a manufacturing tolerance for the pipe wall thickness of +15%, -12.5%. Traditionally, buckling analysis of shells considering imperfect geometry is facilitated by linearly superposing eigemode shapes obtained from a linear eigenvalue buckling analysis. Other approaches include load perturbation and explicit definition of a stress-free imperfection pattern (e.g. [117]). For buried pipelines under compression forces, Yun and Kyriakides [26] report that the presence of even low-magnitude axisymmetric imperfections lowers considerably the bifurcation and limit stress and strains compared to the perfect geometry case. Therefore, care should be taken to reliably establish the initial perturbed geometry of the buried pipeline and apply it on representative shell models. It appears also imperative to examine the combined effect of different imperfection patterns and internal pressure levels on the buckling load of a buried NG pipeline.

Pipe bends

Pipe bends, also known as 'elbows', pose further challenges, as they exhibit more complex behavior compared to straight pipes due to their bent geometry, and can alter the earthquake response of a buried pipeline system. As early as 1979, Shinozuka and Koike [118] used an approximate analytical model of a continuous buried pipeline system to derive the moment- and shear force-induced longitudinal strains developed in right-angle bends and T-junctions under out-of-phase seismic ground motion parallel to one of the legs. Their results show that the more extended the soil-pipe slippage and the larger the seismic wavelength, the larger these strains are (in the first case they can become over twice the free-field strain). McLaughlin and O'Rourke [119] confirm these findings for buried elbows impinged upon by harmonic R-waves, and further support that axial ground strains are an upper bound estimate for the elbow bending strains, except in the case of very thick-walled elbows. Saberi *et al.* [101] studied the effect of various parameters on the bending strains of a right-angle pipe elbow under seismic wave propagation, and concluded that these are maximized for a bend angle of about 135. There are also studies dealing experimentally [120,121] and analytically [107,122] with the static response of soil-embedded pipe bends under PGD-induced in-plane bending. In a review study, Karamanos [123] describes elbows as a critical component of buried pipeline systems because they exhibit more flexible behaviour compared to straight counterparts and are more prone to section ovalization due to bending and fatigue damage under cyclic loading.

3.5 Challenges ahead

Even though it is broadly recognized that classical SSI effects can be safely ignored in a seismically loaded soil-pipe system, contact between soil and pipe should be considered where necessary, as it can differentiate pipe from soil strain. The absence of consensus on the importance of SPI and the relative dispersion observed in calculated pipe demand due to TGD, stem partly from the inability to reliably describe the nonlinear nature of the interaction phenomenon. This has been a subject of continuous research over the years and the substantial progress achieved has provided mainly linear or elastoplastic idealizations of the true nonlinear soil-pipe response. Experimental tests dealing with the derivation of equivalent soil springs are usually based on monotonic loading protocols, and for this reason their applicability can be justified only for cases of earthquake-induced PGD. This, however, overlooks the true cyclic nature of seismic excitation and the hysteretic characteristics of the pipe, the soil and their interface. In view of this, further research is necessary on the development of reliable cyclic force-displacement curves that describe the dynamic SPI under seismic shaking, including contact effects at the soil-pipe interface. Furthermore, what most published SPI models do not reflect is the coupling between the directional components of the relative soil-pipe motion and the subsequent coupling of various failure modes. For instance, it is trivial to realize that when a gap opens in the normal direction of the soil-pipe interface, the frictional behaviour cannot be defined. The same holds for a lateral oblique motion.

Another assumption extensively used is the homogeneity of the medium along the pipeline route, which apparently does not hold true considering that pipelines are geographically distributed systems. Laterally varying soil conditions can profoundly affect stress distribution and magnitudes in the pipeline due to TGD, as already indicated in some studies (e.g. [48,124,125]). This issue also calls for further scrutiny in the framework of dynamic/quasi-static SPI analysis under SVEGM as a result of local site conditions and topography. More importantly, it needs to be clarified whether pipe strains can arise that can lead to critical limit states, such as shell-mode buckling and fracture.

Research so far on the susceptibility of buried pipelines to SVEGM is mostly constrained in analytical boundaries. Further laboratory work is necessary in order to support, calibrate and extend the existing analytical findings. Given that shell-mode buckling is one the most common damage modes observed, particular attention has to be placed on the experimental study of local site effects on the stability of such structures.

4 FRAGILITY OF BURIED STEEL PIPELINES

In the last decades, a gradual transition is seen in the interest of the structural engineering community from conventional deterministic analysis procedures to probabilistic risk assessment concepts, as the understanding of the effect of aleatory and epistemic uncertainty on the response of structures to natural hazards is improved and the computational capabilities are rapidly evolving. Particularly in earthquake engineering, where inherent uncertainties propagate through all stages of assessment and decision-making, structural reliability tools have been widely employed to quantify them, and evaluate the risk level the structure is exposed to. When it comes to the seismic safety of critical civil infrastructure, such as utility systems, probabilistic approaches are deemed necessary to secure minimum functionality disruption and overall longevity under different excitation levels. As outlined in [126], a quantitative seismic risk assessment of oil and gas pipelines involves the following key steps: (a) definition of the physical subject and the objectives of the analysis, which should contain a preliminary (and quite subjective) definition of the target, acceptable risk levels; (b) identification of the expected earthquake hazards and estimation of their likelihood of occurrence, a process that involves many uncertainties and is typically accomplished through probabilistic methods; (c) vulnerability assessment of the pipeline subject by correlating hazard severity to pipeline strain demand and (d) evaluation of the probabilities of occurrence of predefined consequences incurred by pipeline damage.

Because it requires a high degree of expertise and experience to perform, a full seismic risk assessment of buried NG pipelines is generally not required by regulations and is rarely undertaken in practice except a-posteriori, for post-earthquake assessment purposes. Instead, most operators rely on an intermediate output of procedure (c), that is, fragility relationships. In a broad context, fragility expresses the conditional probability that a system or an individual component reaches or exceeds a certain limit damage state for a given level of an intensity measure [127]. Fragility is commonly referred to as the probability of failure, where the term 'failure' does not necessarily imply catastrophic damage, but rather refers to different predefined damage states. In the sphere of earthquake engineering, fragility curves are used to describe the probability that the imposed seismic demand *D* is equal to or greater than the capacity *C* corresponding to a specified damage state of the structure, given a ground motion intensity measure (*IM* hereafter):

$$Fragility = P\left[D \geq C \mid IM\right] \tag{22}$$

Particularly in the context of damage analysis of buried pipelines, probabilistic seismic fragility relations are the typically used evaluation tool, even though they are defined in a much simpler manner compared to those defined for buildings and bridges. They establish a relationship between the spatially distributed pipe damage *rates* and the different degrees of an appropriate *IM*. The damage rate is usually quantified as the pipeline repair rate, i.e. the number of pipe repairs (for breaks or leaks) per unit length of pipelines, although other measures have also been used. Seismic fragility relations are usually categorized according to the damage source type, that is, TGD and PGD, and are expressed in the form of a power law:

$$RR = aIM^{b} \tag{23}$$

where *RR* is the median repair rate and *a*, *b* are parameters estimated by regression analysis of the available data pairs.

Several ground motion IMs have been claimed in the literature to correlate well with pipeline damage, ranging from the standard ones *MMI*, *PGA*, *PGV*, *AI*, $S_a\left(T_1\right)$, to the more pipeline-specific peak ground strain ε_g and PGV^2 / PGA. Most studies on seismic fragility of buried pipelines adhere to the fragility relation scheme based on collected empirical data. At least to the authors' knowledge, only few research efforts [128,129] have advanced to producing classic fragility curves by calculating probabilities of failure rigorously as they are produced, for instance, for the case of bridges [130].

4.1 Empirical seismic fragility relations for buried pipelines

The first studies that utilized observed pipe damage from earthquakes date back to 1975, when Katayama *et al.* [131] published charts of pipe damage as a function of PGA for different soil categories, taking into account data obtained from six events. Later, Eguchi [132] generated expressions for pipe breaks in terms of the MMI scale for various pipe materials, being the first to distinguish between wave propagation and PGD hazards and providing a ranking in terms of vulnerability of different pipe materials as follows (in descending order): concrete, PVC, cast iron, ductile iron, X-grade steel. Barenberg [133] and Ballantyne *et al.* [134] then developed the first fragility relations considering PGV as the ground motion IM. Along the same lines, empirical PGA-based fragility expressions were produced in three subsequent studies [135–137].

A remarkable effort is that of O'Rourke and Ayala [138], who proposed a PGV-based seismic fragility relation based on damage data associated with pipelines of various materials from three earthquake events. Their function concerning damage due to wave propagation was adopted by FEMA in HAZUS methodology [139] and has been thereafter widely used. Further on this subject, O'Rourke *et al.* [140] performed comparative damage analyses using different IMs; their conclusion was that the highest correlation between damage and seismic motion severity is achieved with the use of PGV as IM, that being one of the first confirmations of the enhanced efficiency of velocity- and energy- related IMs, compared to PGA, for problems involving soil response. In an alternative approach, Trifunac and Todorovska [141] defined the damage rate as the amount of pipe breaks per square km of land area and used the peak soil shear strain γ_{max} as IM to derive fragility expressions for water pipelines based on the 1994 Northridge event. O'Rourke and Jeon [142] then used cast iron pipe damage evidence from the 1994 Northridge event to develop a fragility relation for wave propagation. The combined effect of seismic and/or abnormal loadings over time on the fragility of water networks in Cyprus has also been derived by Fragiadakis *et al.* [143].

Because of the major importance of fragility estimates in decision making and lifecycle management of lifelines, the American Lifeline Alliance published guidelines [144] that incorporate the most comprehensive list of seismic fragility relations for water supply pipelines, based on an extensive database of documented damage that includes 81 data points. The relations are provided in the form of backbone functions, allowing for adjustment through correction factors to account for different pipe materials, joint types and other parameters, and their validity has been confirmed in practice in recent earthquake events. It should be noted that the damage data present considerable scatter and, moreover, refer mostly to cast iron (CI) and asbestos cement pipeline. O'Rourke and Deyoe [145] accomplished a twofold objective by re-examining previously used data sets related to segmented buried pipes: on the one hand to illustrate that the peak ground strain ε_g is more consistent than PGV in describing seismic damage to segmented buried pipes, on the other hand to develop improved fragility relations in terms of ε_g. An effort was also made to derive PGV-based relations considering the type of the controlling seismic wave. These relations assume that S-waves govern for near-source sites and R-waves for far-source sites. Jeon and O'Rourke [146] performed comparisons among damage prediction equations using differently estimated PGV, concluding that the maximum recorded PGV value provides better correlation with water supply pipeline damage rates. Later, Pineda and Ordaz [147] proposed a new vector IM for buried pipeline fragility functions, PGV^2 / PGA , and showed that it is more closely related to damage patterns in soft soils. By assuming different effective wave velocity, other researchers [148] presented a revised strain-based fragility relation for segmented pipes exposed to seismic wave propagation.

More recently, Esposito *et al.* [12] presented a comprehensive study analyzing the performance of the L'Aquila medium- and low-pressure gas distribution network in the 2009 earthquake. Relying on damage reports, seismic fragility of buried steel pipes in terms of repair rates was estimated and plotted against local-scale PGV values interpolated using ShakeMaps illustrating the spatial distribution of seismic intensity. Then, the obtained data were validated against existing fragility relations, giving non-negligible damage underestimations by the latter. The deviations were attributed to the fact that the fragility relations used were established for arc-welded steel pipes, while the L'Aquila gas pipeline network consists of gas-welded pipes, which are more vulnerable.

Table 3. Summary of the most recent empirical fragility functions in terms of repair rate (RR/km) for buried pipelines found in the literature; *PGV* in cm/s, K_1 and K_2: correction factors that apply to certain pipe types, *PGD* in cm, ε_g : peak ground strain, *GMPGV*: geometric mean *PGV*

Reference	Fragility function	Applicability
M. J. O' Rourke and Ayala (1989)	$(PGV/50)^{2.67}$	Wave propagation damage
T. D. O'Rourke and Jeon (1999)	$0.00109 \cdot PGV^{1.22}$	Wave propagation damage, CI pipes
ALA (2001)	$K_1 \cdot 0.002416 \cdot PGV$	Wave propagation damage, various pipe typologies
ALA (2001)	$K_2 \cdot 2.5831 \cdot PGD^{0.319}$	PGD damage, various pipe typologies
M. J. O' Rourke and Deyoe (2004)	$513\varepsilon_g^{0.89}$	Wave propagation damage, segmented pipes
M. J. O' Rourke and Deyoe (2004)	$724\varepsilon_g^{0.92}$	Combined wave propagation and PGD damage, segmented pipes
M. J. O' Rourke and Deyoe (2004)	$0.034 \cdot PGV^{0.92}$	Wave propagation damage, surface waves
M. J. O' Rourke and Deyoe (2004)	$0.0035 \cdot PGV^{0.92}$	Wave propagation damage, body waves
M. J. O' Rourke (2009a)	$1905\varepsilon_g^{1.12}$	Wave propagation damage, segmented pipes
T. D. O'Rourke *et al.* (2014)	$10^{-4.52} GMPGV^{2.38}$	Wave propagation damage, CI pipes
T. D. O'Rourke *et al.* (2014)	$0.0839\varepsilon_g + 0.41$	Lateral ground strain damage, CI pipes
M. J. O' Rourke *et al.* (2015)	$2951\varepsilon_g^{1.16}$	Wave propagation damage, segmented pipes

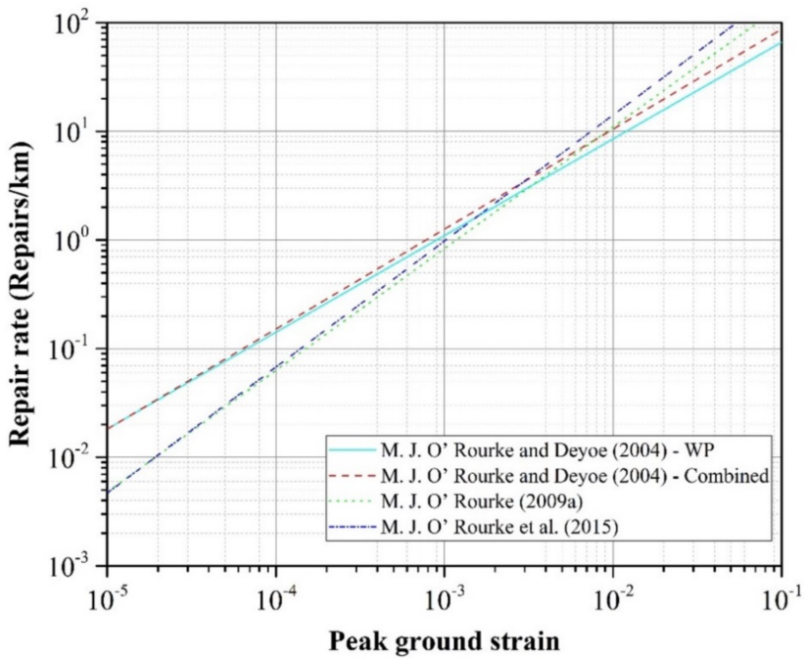

Fig. 11. Comparative log-log plot of published strain-based empirical fragility relations for buried steel pipelines under TGD.

Noteworthy is the fact that high-density polyethylene pipes exhibited no damage at all. More recently, O'Rourke *et al.* [149] assessed the performance of underground water, wastewater and gas pipelines during the 2011 Canterbury seismic sequence. By processing large amounts of damage data through screening criteria, they developed robust fragility relations for different pipe materials, using geometric mean PGV, angular distortion and lateral peak ground strain as IMs. Specifically, for the gas distribution network performance, they comment that it remained almost undamaged, owing to the good ductility of MDPE pipelines. Further, O' Rourke *et al.* [150] enriched the previously proposed fragility expressions [148] with four additional data points obtained from the 1999 Kocaeli event, in Turkey. This fragility relation does not differ significantly from the initial one, hence demonstrating that the latter is fairly stable. Strain-based fragility relations for steel pipelines under TGD are plotted in Figure 11, while all empirical fragility expressions cited herein are summarized in **Table 3**. If we examine Figure 11, we notice that the region of agreement for the plotted curves lies between ground strains of 10^{-3} and 10^{-2}, which are quite large and potentially damaging for the pipeline. Beyond this range, the curves diverge. Of note also, the damage rates increase linearly with the ground strain, a trend that is in contrast with analytical findings [47,96] suggesting that the soil-pipe slippage releases pipeline strain as soon as a relatively small relative displacement is mobilized (of the order of 10^{-3} m). This effect might need to trigger a discussion on the functional form of the fragility curves.

Lanzano *et al.* [128] published one of the few studies that addresses complete fragility curves, in the sense of probability of exceedance of a specific performance level given some measure of ground motion intensity. Their investigation regarded continuous, steel-welded, NG pipelines subject to TGD and the IM used was *PGV* as well. Three discrete damage states were established: slight, significant and severe, which then were associated with corresponding risk states, according to projected estimations of environmental consequences. Utilizing a vast database of past earthquake damage, from which only the well documented cases were considered, seismic fragility curves were developed by fitting the useful data with a lognormal CDF (Figure 12). The extension of this work incorporates fragility curves due to *PGD* [129]. Recently, Melissianos *et al.* [151] presented a probabilistic methodology for performance assessment of fault-crossing buried steel pipelines. Using fault displacement hazard analysis, a vector IM of the fault displacement components and structural analysis of a BNWF pipeline model, they developed fragility surfaces for tensile and compressive strains, with and without account of demand and capacity randomness.

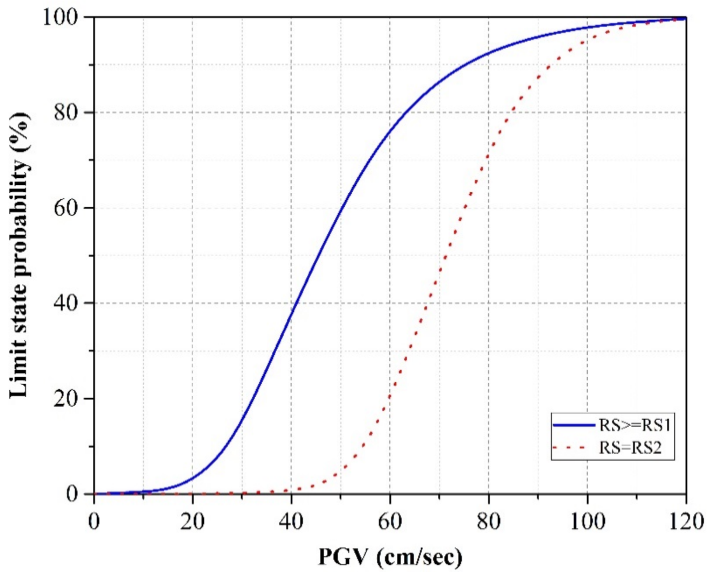

Fig. 12. Seismic fragility curves for buried NG pipelines developed by Lanzano *et al.* (2013) (adapted from [128]). RS1 and RS2 stand for Risk State 1 and 2, corresponding to limited and significant loss of containment respectively.

4.2 Identified challenges

It is evident that the state-of-the-art on seismic fragility of pipelines is limited to empirical expressions, which might be yield more credible damage rates, but their applicability is restricted to cases where ground motion, soil and pipe characteristics are similar to the sample used to derive those simplified expressions. Therefore, generalized and unconditional use into seismic risk assessment, mitigation methodologies and software introduces a significant degree of uncertainty. In light of this fact, analytical fragility curves, verified against experimental results, are expected to provide a more reliable estimate of damage of pipelines under a wider range of seismic scenarios, soil types, and for an extended typology of buried NG pipelines, also allowing for the consideration of special phenomena affecting pipe response, such as the SVEGM and SPI. Damage states have to be explicitly defined and linked to limit state criteria. Further, there seems to be some bias in the available damage information, as most of it concerns segmented water pipelines. Research on vulnerability of continuous steel-welded pipelines, which is the norm in buried NG networks, is scarce; hence, this issue remains to be illuminated.

5 PIPELINE HEALTH MONITORING FOR MAINTENANCE AND REHABILITATION

To achieve the goal of sustainability, two major requirements must be met during the design life of a lifeline: regular maintenance and quick rehabilitation after an extreme event. In this respect, an integral part of the desired service lifecycle of lifelines is the implementation of non-destructive Structural Health Monitoring (SHM) methods during their operation towards the reliable diagnosis of their structural condition. According to Chang [152], SHM provides the means to continuously gather (nearly) real-time information on the integrity of infrastructure without interruption of their service, with the final goal being hazard mitigation. A successful SHM application is typically characterized by the following aspects [153]: (a) almost real-time health screening, (b) minimal service interruption during the monitoring process, (c) deployment of sensing instruments able to capture on a continuous basis variations in specific metrics that determine the state of the structure, (d) transmission of acquired data through an established wired or wireless network and (e) data analysis in order to detect damage patterns and assess damage modes and extent.

SHM has become standard practice for virtually every type of lifeline structure nowadays; underground energy pipelines are no exception to this. Apart from earthquake-induced damage, pipe deterioration may be accelerated by previous time-dependent material degradation and ageing, or even manufacturing defects and imperfections. Pipeline SHM techniques are useful both as a *prevention* tool, in that they can detect on time accumulated damage due to service loads, wearing and pre-existing flaws prior to any failure, and as a *remediation* tool to rapidly localize and characterize incurred damage immediately after the occurrence of an earthquake. Needless to say, the pipeline industry is bound to special regulations that require the implementation of inspection procedures on existing pipelines [154]. Scheduled maintenance by means of visual in situ inspections has now been replaced to a great degree by cutting-edge techniques that not only offer a broader insight of the structure's integrity indicators both in space and in time, but also minimize labor and downtime costs. Excluding the outdated and inefficient in situ inspection, three are currently the main sensing technologies used in pipeline SHM [155]: (a) in-line inspection techniques, (b) fiber optic sensing and (c) remote sensing. Of the three, the first two are the dominant trends in pipeline industry, and for this reason only are treated herein.

5.1 In-line inspection techniques

Perhaps the most widely adopted approach in SHM of buried NG pipelines today is the so-called in-line inspection. Essentially, small autonomous devices known as 'smart pigs' (the term 'pig' derives from Pipeline Inspection Gauge) and carrying sensors, data recorders and transmitters are inserted inside the pipeline and driven by content flow, 'in-line' with it. As they travel long distances in the interior of the pipe, the mounted sensors obtain continuous measurements of various parameters, depending on the desired inspection tasks; these are typically related to geometry checks, strain analysis, metal loss and crack detection. In this manner, large pipeline segments can be examined at reduced times without blocking the transportation process of NG. The basic principle behind the measuring activity that gives meaning to the obtained data is that consecutive measurements are taken over time, thus any change with respect to previously obtained values related to undamaged state will denote a health issue. After proper statistical processing, these data are compared to measurements corresponding to the so-called 'learning' period and diagnosis is then made with respect to the integrity of the pipeline.

Commercially available in-line inspection tools are based on various sensing technologies [155]. Among them, ultrasound-based sensors are common in the market for metal loss and crack inspections. These are sensing transducers that emit ultrasonic pulses in the direction of the pipe wall. The acoustic signals are then reflected from both the inner and the outer wall surface and captured back from the transducer (Figure 13a). From the knowledge of the sound velocity in the medium and by measuring the traveling times of the signal, wall thickness is computed and any metal loss can be inferred. The transducers may be piezo-electric or electro-magnetic, with the latter being the case for NG pipelines as the former require a liquid medium to function, and may also be installed on the external surface of the pipeline. Another highly popular in-line inspection technology tailored to corrosion detection of steel pipelines is magnetic flux leakage. According to the underlying physical principle of magnetization, the inspection unit transmits magnetic flux into the pipe-wall, creating a magnetic circuit. If metal corrosion is present in certain regions, there will be some sort of leakage in the magnetic field, which is detected by magnetic sensors placed on the unit (Figure 13b). Moreover, the latest industry trends suggest the combined utilization of different sensing technologies on a single in-line inspection tool in order to carry out more reliable, multi-purpose pipeline inspections.

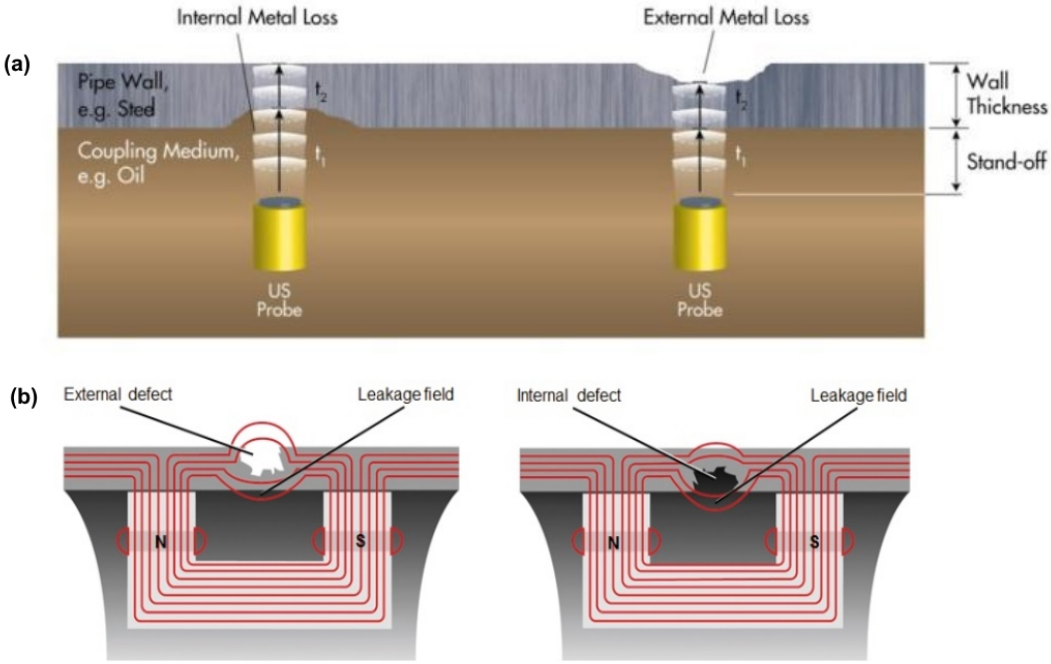

Fig. 13. Schematic views of in-line inspection technologies: (a) principle of ultra-sound based sensors (reprinted from [154]; (b) principle of magnetic flux leakage sensors

5.2 Distributed fiber optic sensing

Fiber optic sensors are one of the most promising technological developments in the field of SHM, although their first use can be traced back as early as the 1970s [155]. The function of fiber optic systems is based on the physical properties of light propagation: the goal is to associate unexpected variations in the light signals as they travel along fiber strands with damage patterns. Through various configurations, fiber optic sensing offers diverse capabilities in measuring a number of different parameters, including strain, temperature, pressure and acceleration [153]. What is of interest in examining the condition of a pipeline subject to earthquake effects is primarily the strain levels in the pipeline. Discrete and, lately, distributed fiber optic sensors have been used for strain monitoring purposes. Although discrete sensors provide unmatched resolution and accuracy in local-scale measurements, they are not suitable for global monitoring, as this would require the installation of thousands of them along the pipeline, together with a complex wiring system, leading to prohibitively high costs.

This significant drawback is surmounted by the distributed fiber optic sensors, which are capable of efficiently monitoring large portions of such elongated systems as pipelines. Distributed sensors are fairly simple in their structure; they comprise a single silicon fiber cable sensitive at its whole length, which is tightly bonded to the pipe wall upon installation in order to allow lossless transfer of the material strains. Low attenuation levels ensure that distributed sensors perform well over distances of up to 25 km [156]. Other advantages of the distributed sensing technology include simple cable connections to the data receiver and reduced installation effort and cost.

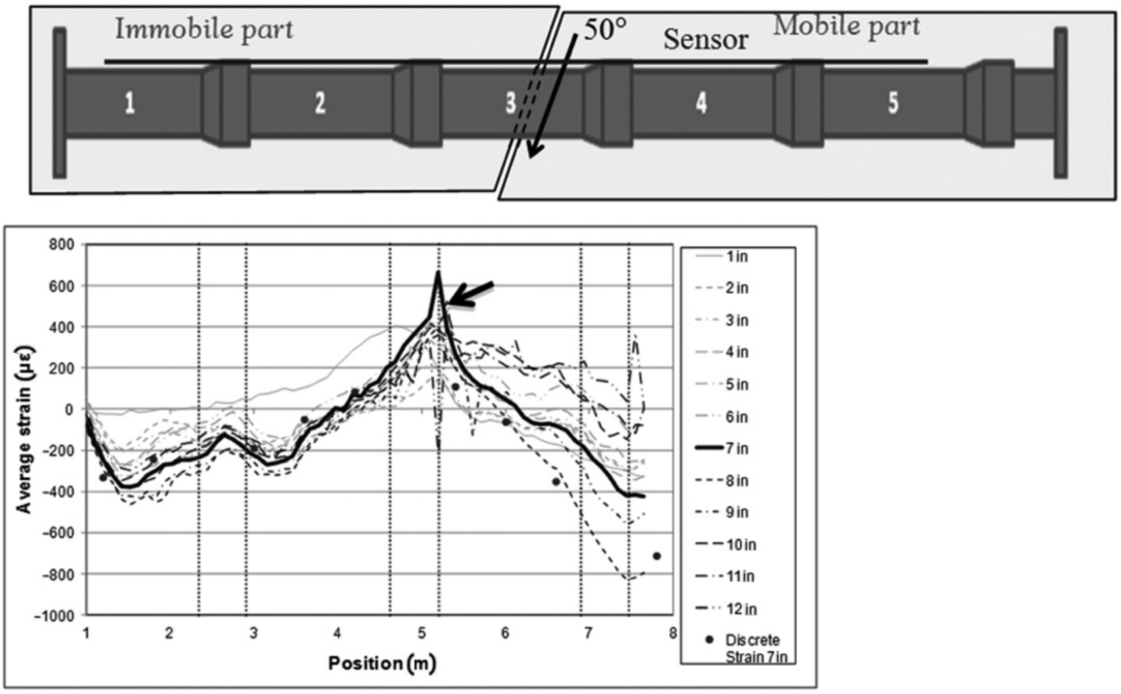

Fig. 14. Select results from the pipe strain monitoring experiment with distributed Brillouin sensors conducted by Glisic and Yao (2012), indicating detected damage inside the strain concentration region (reprinted from [157]).

Distributed fiber sensing technology relies on one of the following three optical effects: Rayleigh scattering [158], Raman scattering [159] and Brillouin scattering [160]. Technical details about these fall out of the scope of this study and may be found in the relevant references. Brillouin scattering-based implementations are usually the method of choice, since they suffer the least from signal losses and they are capable of long-range monitoring [157]. Several experimental studies have been conducted that demonstrate the effectiveness of the method. For instance, Inaudi and Glisic [156] present the results of the field application of a previously developed Brillouin distributed strain, temperature and combined strain-temperature sensing instrument (DiTeSt) [161]. Excellent performance of distributed strain monitoring on a buried gas pipeline subjected to landslide loading was reported, as well as successful detection of the leakage spot by the distributed temperature sensors during a gas leakage simulation. In an earlier laboratory test, Ravet *et al.* [162] took advantage of the unique capability of distributed Brillouin sensors to measure both tension and compression at the same time, in order to detect the starting point of buckling in a steel pipe under axial compressive load. To ensure prior knowledge of the location of buckling initiation, weakening of the specimen wall was performed at a specific region. Comparison between the measurements from the distributed Brillouin sensor and installed strain gauges along the pipe body showed good agreement, and tensile strains were successfully detected by the distributed Brillouin sensor, signifying the initiation of the buckling process. Glisic and Yao [157] put extensive efforts in developing an integrated damage monitoring method of buried concrete segmented pipelines exposed to seismic effects, using distributed Brillouin scattering-based fiber optic sensors. In validating the method with large-scale testing, PGD was simulated to act on a 13 m-long pipeline assembled inside a test basin and covered with soil, while strain readings obtained from the fiber optic sensors were verified against data from conventional strain gauges (Figure 14). Damage accumulation in the joints was mainly observed, as expected, and the sensing system achieved to identify these patterns as strain peaks in the strain profiles. The applicability of the method can be safely extended to continuous steel pipelines according to the authors.

5.3 Critical summary and SHM issues to be addressed

The aforementioned pipeline inspection techniques are not universally applicable in industrial practice, as they present specific drawbacks that limit their implementation. A crucial factor that determines the suitability of in-line inspection tools is the potential of the pipeline to permit passage of the 'pig' unit through its body (known as 'pigability'), which depends on a number of pipeline attributes, such as the size of the pipe section, the operational pressure and the flow conditions [163]. Besides, in-line inspection requires some degree of manual operation, as well as efficient energy management of the wireless sensors. More importantly, in-line inspection techniques are considered less suitable than distributed fiber optic sensing for emergency-state rapid damage detection following an earthquake, as they require longer operating times. On the other hand, fiber optic solutions are particularly expensive, and their cost tends to increase dramatically with higher measurement accuracy. Distributed fiber sensors also require more intricate installation procedures and ensuring of good bonding with the pipe wall is a prerequisite for accurate sensor readings; further to this, optimized placement of the distributed sensors on the pipe circumference is another concern for reliable integrity monitoring [164].

As a general remark concerning the full spectrum of available inspection technologies, it should first be underlined that, like above-ground structures, there is great computational demand in handling effectively the vast amount of data that are acquired from long-term pipeline monitoring facilities. To this end, efforts should be made towards the development of efficient data processing tools that incorporate sophisticated threshold-based algorithms of deterministic or statistical background, to reliably interpret captured metrics variations on the basis of previous samples. Second, the major challenge is to take advantage of the existing pipeline SHM technologies in a holistic approach involving rapid post-rupture health assessment, fast repair actions and decision-making in the direction of network resilience. Such considerations should not ignore the fact that, during a post-earthquake crisis period, power supply and wireless communications networks may experience long-lasting outages, hence hindering any integrity assessment works. The same applies to accessibility issues attributed to landslides and road network disruption.

6 THE EMERGING CONCEPT OF RESILIENCE IN PIPELINE NETWORKS

Resilience is a rapidly-developing concept in the domain of lifeline engineering that can be understood in the context of emergency situations caused by natural (e.g. earthquakes, floods, hurricanes) or manmade (e.g. vehicle collisions, bomb explosions) extreme events that induce abrupt variations in the performance of lifelines. Even though there is a breadth of different definitions spreading along different disciplines, in an earthquake engineering context resilience denotes the highly desirable property of either a physical infrastructure or a social (community) system that relies on engineering works to adapt to and recover fast from a disruptive or disastrous event. Naturally, it requires multidisciplinary considerations for its quantification as it draws knowledge from seismology, earthquake (geotechnical and structural) engineering, economics, social and management sciences, among others.

6.1 Analytical treatment of resilience

In a pioneer work, Bruneau *et al.* [165] set the foundations for the quantitative assessment of seismic resilience. They define a resilient system as one that obeys to three basic rules:

- It is characterized by enhanced reliability.
- It generates tolerable levels of losses when experiencing failure.
- It can return quickly to a previous performance standard after failure.

The preliminary identification of these core features of resilience are a prerequisite to its quantification. Drawing upon a study by Cimellaro *et al.* [166], seismic resilience is expressed as an index R that represents the capacity of an infrastructure system or community to withstand earthquake effects by retaining an acceptable level of performance over a given post-earthquake time period, through a process involving loss estimation, collection of resources, relief strategy planning and restoration actions. The time-dependent performance of the system is measured in terms of functionality $Q(t)$, a dimensionless function of time, denoting the service quality of an infrastructure system at any time instant as a proportion of the full functionality corresponding to the initial, intact state of the system, assumed to be equal to 100% (Figure 15). A mathematical definition of seismic resilience under the consideration of a single seismic event is possible:

$$R = \frac{1}{t_h - t_0} \int_{t_0}^{t_h} Q(t)\, dt \tag{24}$$

where t_0 is the time of the occurrence of the seismic event and t_h is the investigated time horizon. Graphically, eq. (24) represents the shaded area underneath $Q(t)$ over the time interval $t_h - t_0$, normalized with respect to this interval, as illustrated in Figure 15. The mathematical definition of functionality involved in Eq. (24) may vary depending on the system examined. In general, it can be based on qualitative or ranking measures, which provide the means to represent the consequences of some specific damage level (input) on the functionality of the system (output). Alternatively, it can be modelled as a non-stationary stochastic process [166].

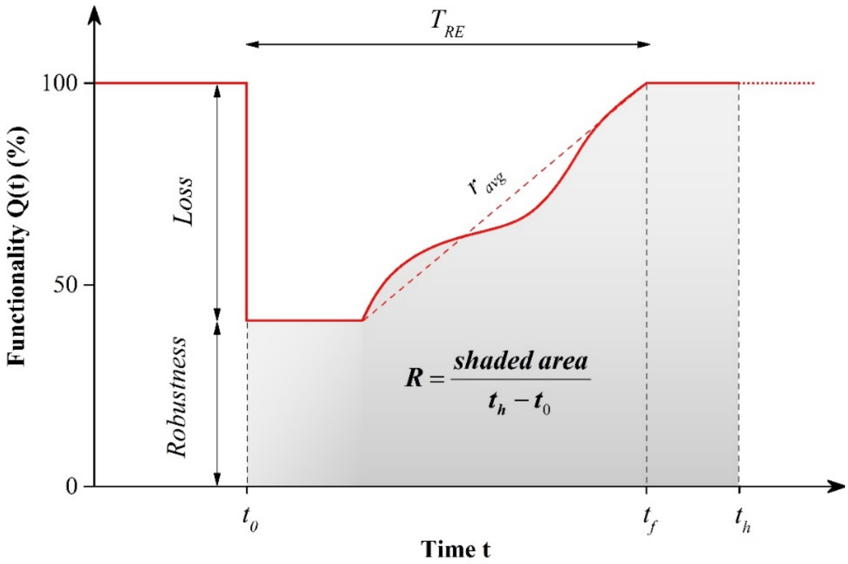

Fig. 15. Graphical illustration of time-varying functionality, resilience, rapidity and robustness; *R*: resilience; r_{avg} : average rapidity; T_{RE} : recovery time

6.2 Dimensions of resilience

Establishing a quantitative definition of resilience is not straightforward, while its evaluation and enhancement pose an additional challenge, given the various sources of uncertainty that arise and the subjectivity of the problem. As Bruneau *et al.* [167] propose, this task can be facilitated if the idea of resilience is broken down into simpler descriptors: (a) rapidity, (b) robustness, (c) redundancy and (d) resourcefulness. Detailed descriptions of these quantities are available in Refs. [167,168]. Rapidity and robustness are quantifiable (refer to Figure 16), while redundancy and resourcefulness are more abstract qualities of an infrastructure system, difficult to quantify and also interlinked with each other. To make a distinction from rapidity and robustness, redundancy and resourcefulness provide the means to achieve resilience, whereas rapidity and robustness are descriptors of the final outcome.

6.3 Seismic resilience assessment of buried NG networks

Some key considerations and existing research on seismic resilience of buried NG networks are discussed in this section.

Seismic hazard analysis

Similar to seismic risk assessment, seismic hazard analysis forms an integral part of seismic resilience assessment, as it provides essential input (i.e., IM distribution) to the loss estimation process. Because of the spatial correlation of the ground motion across different network stations [169], it would be irrational to construct regional seismic hazard maps based on methods that account for the seismicity of multiple sources. In this case, the problem is usually addressed by considering single seismic scenarios derived deterministically or from disaggregation of PSHA-generated seismic hazard maps. Another approach is proposed by Sextos *et al.* [170], where seismic scenarios associated with specific return periods are produced by PSHA for each seismic source independently. Appropriate IMs for assessing pipeline network loss are discussed in Section 4.

Loss estimation

In loss estimation, a major difficulty is that there is correlation between direct and indirect loss in NG networks because flow disruption in one network component effectively impedes the functionality of all downstream components. NG pipeline networks are generally not characterized redundant, hence flow redistribution is usually impossible. More importantly, given that NG networks also supply energy to power plants, the indirect losses stemming from a potential general power outage can be elusively high. This implication may severely slow down the emergency response, the recovery activities and the rehabilitation process of the damaged network component, and consequently lead to a costly vicious circle. The strong interdependence between modern life aspects and the uncertainty in identifying and quantifying losses relating to different domains (e.g. economy, society, and environment) adds to the complexity of the indirect loss estimation, which is still hard to perform in a reliable quantitative manner. Moreover, in contrast to the immediate direct loss, indirect loss can grow or shrink during the gradual restoration of pre-event functionality. Ageing effects, such as corrosion, and previous undetected structural defects or damage can further impact resilience levels by downgrading the initial state of functionality and also increasing the immediate functionality drop down to the residual level right after the natural disaster, a fact that most often goes unnoticed. For these reasons, only a wider network analysis of the consecutive recovery phases can capture the time evolution of the indirect losses and give a reliable estimate overall.

Risk mitigation strategies

Another consideration with elevated meaning to resilience enhancement is the risk mitigation strategies. A distinction between pre- and post-earthquake mitigation measures is meaningful here. Pre-earthquake measures are usually implemented in the design phase of a pipeline network and aim to either reduce the friction at the soil-pipe interface, hence eliminate pipe axial stress development, increase pipe stiffness or strength, hence reduce deformation, or increase flexibility, hence accommodate deformation. Some common 'mild' measures of this type applied in practice to minimize PGD effects in critical regions are the following: wrapping of the pipeline with geotextiles, use of low-friction coatings, encasement of pipeline into isolation concrete culverts, backfilling with loose material, trench widening. These can prove to be effective also when TGD is the main geohazard, particularly in regions of sharp changes in the ground stiffness or topography. Other more drastic preventative measures include use of flexible joints and above-ground elevation or re-routing of a pipeline portion to avoid hazardous land zones, the latter rarely being an option due to right-of-way permissions. A more comprehensive list of such measures can be found, among others, in [126,171,172]. In [171], a comparative quantitative evaluation of alternative measures is also presented, and it is found that geotextile fabrics, pipe wall thickness increase and trench backfilling with loose soil provide rather low to moderate protection, while concrete culverts appear more effective. The effectiveness of each preventative measure reflects directly on the residual functionality following a seismic event (i.e., robustness), and implicitly has effect on the recovery time.

Post-earthquake measures refer to rapid repair actions taken just after the event and long-term rehabilitation strategies to restore near-initial functionality of the network. For instance, the currently operating NG network rapid response and risk mitigation system in Istanbul [173] will interrupt NG flow if threshold IM values are exceeded upon reception of early-warning system signals. Subsequently, the deployed array of strong motion recording instruments generates real-time regional hazard maps, and the distribution of damage in the pipeline network is estimated using fragility relations soon after the earthquake strikes. Based on these, decision-makers are ready to prioritize rapid repair where necessary. Cimelarro *et al.* [174] test a NG network retrofit system consisting of automatic seismic gas shutoff valves, flow dividers and valves located in compressor stations. Analysis for different seismic scenarios show that it augments resilience by an average of 78%. The effect of each remediation measure on the recovery time of the network remains to be investigated, so that designers and stakeholders gain understanding into the techno-economic trade-off of each measure. Distributed fiber optic sensors (Section 5.2) appear a promising solution for rapid health screening of a NG network and their efficiency should be evaluated for resilience enhancement purposes.

Latest research

Only a handful of studies on quantitative evaluation of seismic risk and resilience are on record, since it is a topic that has gained scientific interest quite recently [175]. Esposito *et al.* [12] analyzed the time-evolution of network functionality described in terms of the ratio of reconnected customers over total customers after the shock, showing that only 40% of the customers were reconnected to gas supply after two months. The low restoration level achieved is attributed to the fact that reconnection was permitted only to buildings that received a green-tag during post-earthquake inspection. More recently, Cimelarro *et al.* [174] developed and applied to a case study a comprehensive quantitative framework for the seismic risk analysis of gas distribution networks considering the impacted network functionality and the ensuing recovery process. Network functionality defined as a function of the time-variant gas flow and total operating pipe length was computed with numerical modeling using SynerGEE software. A single seismic scenario was extracted by de-aggregating local hazard maps corresponding to 22% probability of exceedance in 50 years and median PGV maps were calculated using attenuation relationships. Only PGD-induced pipe damage was considered and the ALA fragility relations were exploited to express pipe damage distribution in a repair rate format. The study resulted in the estimation of resilience indices of the gas network for all damage scenarios, before and after the application of a retrofit alternative, including emergency shutoff valves and flow dividers.

In the same spirit, but for different network type, Dong and Frangopol [176] presented a resilience assessment methodology for highway bridge networks under mainshock and aftershock effects, introducing a probabilistic post-event functionality metric that is a function of damage state indices and bridge fragility. Resilience is estimated from Eq. (24) by using appropriate normal CDFs to model the recovery phase, depending on the damage state. In Sextos *et al.* [170], where intercity networks are addressed, resilience-centered time-dependent qualitative loss indicators of binary form are introduced to track the over-time variation of direct and indirect losses not easily quantifiable in monetary terms (here: connectivity, accessibility, environment), and their effect on the functionality metric. The previous two approaches are examples of transportation networks linking structural, geotechnical with network and consequence analysis that can be potentially adapted to the case of pipeline networks after appropriate modifications.

7 CURRENT CODES OF PRACTICE AND GUIDELINES FOR EARTHQUAKE-RESISTANT DESIGN OF BURIED PIPELINES

Presently, few modern codes and standards worldwide dictate requirements for the protection of underground NG pipelines against seismic risk, the most notable being Eurocode 8 - Part 4 [38] in the European Union, the American Lifeline Alliance guideline [66] in the U.S. and the design recommendations by Japan Gas Association [37]. In this section, the key points in each normative document are discussed. It should be made clear that seismic loading is not a primary consideration in design of pipeline sections, rather it is the flow capacity and the internal pressure that dictate the selection of diameter, thickness and steel grade.

7.1 Eurocode 8 provisions (2006)

Part 4 of Eurocode 8 [38] provides a broad regulatory framework for the seismic design of pipelines, inter alias. According to it, the ultimate limit state of a pipeline is associated with structural collapse. Yet, it is implied that certain critical components of the system susceptible to brittle failure may be checked for a state prior to total failure. A two-level serviceability limit state hierarchy is prescribed; the lower one requires that the system remains fully operational and leak-proof and the higher one that it undergoes some level of damage without losing its whole supplying capacity. Another secondary safety hazard that should be taken into consideration in ultimate limit state (ULS) design is explosion and fire in the event of an earthquake-induced breakage and the potential consequences on people and the environment. The determination of the seismic actions should be based on the two principal sources of damage, i.e., TGD and PGD.

Further, Eurocode 8 states that pipe inertial forces related to ground acceleration are of minor significance in comparison with the forces caused by ground deformation, thus they may be neglected; this simplifies the nature of the problem, converting it to a static one. With regard to wave propagation effects, Annex B of Eurocode 8 recommends the conservative method developed by Newmark [52] to determine the induced pipe strains and curvatures, as long as the soil is stable and homogeneous. As for the spatial variability in ground motion, no particular guideline is provided; however, in the chapter concerning above-ground pipelines, it is suggested that spatial variability is accounted for when the pipeline length analyzed is over 600 m or the ground is characterized by longitudinal non-uniformities. It is also noted that pipelines buried in dense soil are allowed to be designed solely for the effects of wave propagation.

For steel welded pipelines, Eurocode 8 specifies that the maximum ductility of steel is not exceeded and buckling modes are not observed. For the first condition, ultimate steel tensile strain is set to 3%; for the second, the allowable steel compressive strain is proposed as the smaller value between 1% and $20(t/r)$, where *t* is the thickness and *r* the radius of the pipe.

7.2 American Lifelines Alliance guidelines (2001)

The report prepared by American Lifelines Alliance (ALA) [66] focuses on roughly the same points with Eurocode 8. In addition, it suggests performing three-dimensional nonlinear quasi-static FE analysis for investigating PGD effects, considering soil-pipeline interaction. The mechanical behavior of both the steel pipe and the soil should be modeled as inelastic. The length of the pipeline model should be carefully selected in a way that the imposed constraints at the ends do not produce unrealistic local axial deformations. The need to ensure a more refined mesh in the proximity of the PGD region is also highlighted.

In terms of modeling of wave propagation effects, it is stressed that flexural strains may be neglected, due to being much smaller than axial ones. Moreover, the conservative assumption that soil strains are caused by surface waves can be adopted, since this results in larger strains. Wave propagation-induced soil strains are usually expected to be lower than 0.3%.

A list of performance criteria are proposed, which, however, are not universally applicable; different permissible values may be set for each specific case. For PGD-induced axial strains, two performance states are suggested: operable state and pressure integrity state. For the first, non-exceedance is dictated of a 2% tensile strain and a limit compressive strain defined as

$$\varepsilon_{c,cr} = 0.50\left(\frac{t}{D'}\right) - 0.0025 + 3000\left(\frac{pD}{2Et}\right)^2 \tag{25}$$

where $D' = D\big/\left[1 - 3\big/D\left(D - D_{\min}\right)\right]$ and $D_{\min}$ is the minimum measured diameter due to ovalization. Eq. (25) was proposed by Gresnigt [41]. The corresponding limits for the second are $\varepsilon_{t,cr} = 4\%$ and $\varepsilon_{c,cr} = 1.76t / D$. Concerning the effects of wave propagation, the resulting bending stress must not exceed the yield strength of steel. The allowable tensile strain is set to 0.5%, while the allowable compressive strain is defined as 3/4 of the limit specified in Eq. (25). All above limits are in force only on the condition that strict welding procedures are adopted during construction of the pipeline. The soil spring relationships discussed in Section 3.1.2 are proposed. It is noted that the calculation of axial springs must be performed considering backfill soil properties.

7.3 Recommended practice by Japan Gas Association (2000)

The ‘Recommended practice for earthquake-resistant design of gas pipelines’ developed by Japan Gas Association (JGA) [37] constitutes a revised version of the initial guideline, issued in 1982. It features a strict methodology for designing high-pressure transmission pipelines to Level 2 seismic motions. Design seismic motions are specified based on two performance levels similar to Eurocode 8: Level 1 states that ‘operation can be resumed immediately without any repair’, while Level 2 states that ‘the pipeline does not leak, though deformed’. The design flow comprises two phases. In the first phase, the design seismic motion is determined considering the potential existence of active faults near the pipeline route, which may require a fault analysis. The second phase consists of a sequence of simplified formulas that estimate wave propagation-induced pipe strains. Specifically, the natural period of vibration T of the surface soil layer and then the apparent wavelength of the assumed seismic motion are calculated first:

$$T = 4H/\bar{V}_s \tag{26}$$

where H is the thickness of the layer and $\bar{V}_s$ the weighted S-wave velocity,

$$\ell = V_{app}T \tag{27}$$

where V_{app} is the apparent wave propagation velocity of the motion. Following is the calculation of the axial ground displacement U_h at the depth of the pipe axis as

$$U_h = \frac{2}{\pi^2} c \cdot T \cdot S_V \cos\left(\frac{\pi z}{2H}\right) \tag{28}$$

where c is the seismic zone coefficient, S_V the spectral velocity of the soil layer and z the pipe burial depth. The peak ground strain of uniform, regular ground can then be estimated:

$$\varepsilon_g = 2\pi U_h/\ell \tag{29}$$

The last step involves extraction of the pipe strain from the ground strain using a strain transfer coefficient

$$a = q\frac{1}{1+\left(\frac{2\pi}{\ell}\right)^2 \frac{\mathrm{EA}}{k_a}} \tag{30}$$

where q is a coefficient accounting for soil-pipe sliding and k_a is the axial soil spring stiffness. Finally, pipe strain is calculated as

$$\varepsilon = \alpha \cdot \varepsilon_g \tag{31}$$

and checked against an allowable strain of 3%. The previous procedure applies to straight pipe segments, provided that no fault affects the pipeline; a slightly different last step is proposed for pipe elbows and tees.

7.4 Other design guidelines

Other standards and regulations provide hardly any additional useful information on the issue. The B31 Code for Pressure Piping by the ASME [177,178] highlights that the maximum axial stress for a restrained pipeline should be constrained up to a level that no buckling is caused; the permissible value for the sum of all the longitudinal stresses is established as

$$\sigma_{\alpha,\max} = 0.90\sigma_y \tag{32}$$

Axial strain should not develop further than 2%. Furthermore, design against for soil liquefaction and landslides should be performed based on the operability performance level.

A relevant report by FEMA [21] states among others that, unless previously corroded or poorly assembled, buried pipeline systems are quite unlikely to get largely affected by traveling seismic waves; on the other hand, permanent ground deformations are considered to have a higher damaging potential. Increasing the ductility capacity of the pipeline and ensuring protection against corrosion and high quality welding are qualified as capable measures to improve the performance of the pipeline even under large permanent ground movements.

7.5 Observations

Except for JGA guidelines, existing codes are not seen to provide a concrete framework for earthquake-resistant design or seismic performance assessment of buried steel pipelines, rather their utility is limited to coarse tips and recommendations on construction practices and simplifying assumptions. Eurocode 8 insists on the conditionally reliable but outdated method by Newmark, disregarding the long recognized SPI influence on pipe response. ALA goes one step further by proposing soil spring relationships; their applicability, however, has limitations as discussed previously. On the other hand, JGA does define a specific methodology for design of buried pipes solely against wave propagation, but this considers only axial response and homogeneous soil; in addition, it does not address the question of what soil spring constants should be used.

Overall, the previous guidelines are far from comprehensive and do not yet make use of the breadth of research observations, methods and data reported in the literature. More importantly, striking is the total absence of any reference to vulnerability assessment and seismic risk or resilience of gas networks. Focus is made on the component level instead of the network level. Similarly, no information is provided on SVEGM and SHM techniques.

8 DISCUSSION AND CONCLUSIONS

This review study provides a critical discussion on the state-of-the-art in seismic analysis, safety verifications and resilience assessment of buried steel NG pipelines through an integrated treatment of the most significant relevant aspects. Conclusions and challenges can be summarized as follows:

- Current performance criteria for TGD actions, especially those for more complex damage modes, such as buckling, seem to lack concrete support by experimental findings. Efforts should be directed towards dynamic SPI tests to develop more reliable limit state parameters, considering all important factors controlling the dominant damage modes. Criteria for potential interaction of different damage modes would be valuable as well, as a combined damage mechanism might be more detrimental.
- The true cyclic pattern of TGD has been mostly overlooked in previous SPI analyses. It should be verified whether experiment-validated cyclic spring models displaying hysteretic loops offer advantage over the commonly used elastic-perfectly plastic ones in dynamic BNWF model simulations. Coupling between different SPI directions is generally not considered in current equivalent spring models. 3D continuum models, although computationally expensive, are essential to explore the buckling capacity of buried pipelines, and to further our understanding into the influence of various parameters, such as the contact models, pre-load conditions, initial imperfections and internal pressure. Pipe axial trains only due to wave passage are usually found to be way below the 0.5% yield limit of API 5L steel. In light of this, site-specific analyses, considering the most unfavourable ground conditions (horizontal variation of soil stiffness/irregular topography) crossed by the pipeline, are deemed necessary to obtain the most critical pipe demand under local site effects. This approach should be reflected in the relevant codes. Physical testing would be of value in order to verify and extend analytical findings.
- Current knowledge on seismic fragility of buried steel pipelines need be expanded beyond the simplified expressions of repair rates based on both computational and experimental investigation of the limit states for the various modes of failure relating to the integrity of a pipeline. This will also allow the examination of the effect of SPI and SVEGM on pipeline damage rates.
- Two are the predominant pipeline SHM methods used in practice today: in-line inspection and distributed fiber sensors. Both exhibit benefits and drawbacks in different perspectives, though fiber-based monitoring appears to be a more attractive option in the long term. The challenge here is to efficiently utilize them in post-earthquake health screening to maximize rapidity of recovery and consequently resilience levels.
- Seismic resilience of buried NG networks is still an open issue. Resilience levels depend on pipeline robustness, which in turn depends on the network vulnerability; the latter exhibits dependence on various factors, such as seismic hazard definition, pipeline demand and earthquake protection measures. Resilience is also affected by rapidity in post-disaster response, which can be

improved through better SHM and emergency preparedness, and redundancy, which is generally not an inherent property of NG networks. All these interdependencies need to be scrutinized in order to proceed to the development of reliable seismic resilience assessment methodologies. These methodologies shall arrive at specific indices that can support the informed decision-making of the stakeholders. The effect of pre- and post-event mitigation measures on the resilience levels of the network must be comparatively assessed.

- Modern seismic standards and guidelines do not yet reflect important findings of the latest state-of-the-art in research. The existing provisions for TGD actions mainly concern the wave passage effect, which however is rarely critical to the pipeline integrity. There is also a general lack of a detailed step-by-step design methodology that will guide the practicing engineer throughout the process of seismic design. In contrast, a set of empirical recommendations are mainly provided, which however are sometimes incomplete or outdated. Last but not least, there is a lack of a holistic strategy for the resilience-based management of a NG pipeline network towards disaster risk mitigation at large.

Acknowledgements

This work was supported by the Horizon 2020 Programme of the European Commission under the MSCA-RISE-2015-691213-EXCHANGE-Risk grant (Experimental & Computational Hybrid Assessment of NG Pipelines Exposed to Seismic Risk, www.exchange-risk.eu). This support is gratefully acknowledged. The first author would also like to express his gratitude to the Engineering and Physical Sciences Research Council (EPSRC) for financially supporting his doctoral studies. We are also thankful to the anonymous reviewers whose constructive comments helped towards the improvement of this manuscript.

References

[1] REGULATION (EU) No 994/2010 OF THE EUROPEAN PARLIAMENT AND OF THE COUNCIL of 20 October 2010 concerning measures to safeguard security of gas supply and repealing Council Directive 2004/67/EC. Off J Eur Union 2010:1–22.
[2] International Energy Agency. World energy outlook 2015. 2015.
[3] S.M. Folga. Natural Gas Pipeline Technology Overview. Environ Sci Div 2007. doi:ANL/EVS/TM/08-5.
[4] O'Rourke TD, Palmer MC. Earthquake performance of gas transmission pipelines. Earthq Spectra 1996;12:493–527.
[5] Chen WW, Shih B, Chen Y-C, Hung J-H, Hwang HH. Seismic response of natural gas and water pipelines in the Ji-Ji earthquake. Soil Dyn Earthq Eng 2002;22:1209–14. doi:10.1016/S0267-7261(02)00149-5.
[6] Sakurai A, Takanashi T. Dynamic Stresses of Underground Pipelines During Earthquakes. Proceed. 4th World Conf. Earthq. Engng., Santiago, Chile: 1969, p. 81.
[7] Housner GW, Jenningst PC. The san fernando california earthquake 1972;1:5–31. doi:10.1002/eqe.4290010103.
[8] Benfer NA, Coffman JL. San Fernando, California Earthquake of Feb. 9, 1971. Washington DC: 1974.
[9] Hall JF, Holmes WT, Somers P, Institute EER. Northridge earthquake of January 17, 1994: reconnaissance report. Earthquake Engineering Research Institute; 1996.
[10] EQE Summary Report. The January 17, 1995 Kobe Earthquake. 1995.
[11] O'Rourke MJ. Wave Propagation Damage to Continuous Pipe. Tech. Counc. Lifeline Earthq. Eng. Conf. (TCLEE), Oakland, CA, June 28-July 1., Reston, VA: American Society of Civil Engineers; 2009. doi:10.1061/41050(357)76.
[12] Esposito S, Giovinazzi S, Elefante L, Iervolino I. Performance of the L ' Aquila (central Italy) gas distribution network in the 2009 (M w 6 . 3) earthquake 2013;2009:2447–66. doi:10.1007/s10518-013-9478-8.
[13] Koike T, Mori S, Chiba K. Seismic performance assessment of the transmission pipeline after the 2011 great east Japan earthquake 2013:2287–94.

[14] Ariman T, Muleski GE. A Review of the Response of Buried Pipelines Under Seismic Excitations. Earthq Eng Struct Dyn 1981;9:133–51. doi:OO98-8847/81/020133-19%01.OO.
[15] Datta TKK. Seismic response of buried pipelines: a state-of-the-art review. Nucl Eng Des 1999;192:271–84. doi:10.1016/S0029-5493(99)00113-2.
[16] Liang J, Sun S. Site Effects on Seismic Behavior of Pipelines : A Review. J Press Vessel Technol 2000;122:469–75.
[17] Pineda-Porras O, Najafi M. Seismic Damage Estimation for Buried Pipelines : Challenges after Three Decades of Progress. J Pipeline Syst Eng Pract 2010;1:19–24.
[18] Manolis GD, Beskos DE. Underground and lifeline structures. In: Beskos DE, Anagnostopoulos SA, editors. Comput. Anal. Des. Earthq. Resist. Struct. A Handb., Southampton: Computational Mechanics Publications; 1997, p. 775–837.
[19] Hashash YMA, Hook JJ, Schmidt B, I-Chiang Yao J. Seismic design and analysis of underground structures. Tunn Undergr Sp Technol 2001;16:247–93. doi:10.1016/S0886-7798(01)00051-7.
[20] O'Rourke MJ, Liu X. Response of Buried Pipelines Subject to Earthquake Effects. 1999.
[21] Yokel FY, Mathey RG. Earthquake Resistant Construction of Gas and Liquid Fuel Pipeline Systems Serving, or Regulated by, the Federal Government 1992.
[22] Kyriakides S, Corona E. Plastic Buckling and Collapse Under Axial Compression. Mech. Offshore Pipelines Buckling Collapse, Vol. I, 2007, p. 280–318. doi:http://dx.doi.org/10.1016/B978-008046732-0/50011-8.
[23] Vazouras P, Karamanos S, Dakoulas P. Finite element analysis of buried steel pipelines under strike-slip fault displacements. Soil Dyn Earthq Eng 2010;30:1361–76. doi:10.1016/j.soildyn.2010.06.011.
[24] Chen CC, Ariman T, Lee LHN. Buckling Analysis of Buried Pipelines Under Seismic Loads. Proc. 7th Eur. Conf. Earthq. Engng, 1980, p. 249–256.
[25] Lee LNH, Ariman T, Chen CC. Elastic-plastic buckling of buried pipelines by seismic excitation. Int J Soil Dyn Earthq Eng 1984;3:168–73. doi:10.1016/0261-7277(84)90032-9.
[26] Yun H, Kyriakides S. On the beam and shell modes of buckling of buried pipelines. Soil Dyn Earthq Eng 1990;9:179–93. doi:10.1016/S0267-7261(05)80009-0.
[27] Hall WJ, Newmark NM. SEISMIC DESIGN CRITERIA FOR PIPELINES AND FACILITIES. 1977:18–34.
[28] ASCE Technical Council on Lifeline Earthquake Engineering. Guidelines for the seismic design of oil and gas pipeline systems. New York, N.Y.: American Society of Civil Engineers; 1984.
[29] McNorgan JD. Relieving Seismic Stresses Locked in Gas Pipelines. Proc. Second U.S.-Japan Work. Liq. Large Gr. Deform. Their Eff. Lifelines, Buffalo, New York: Technical Report NCEER-89-0032, Multidisciplinary Center for Earthquake Engineering Research; 1989, p. 363–9.
[30] Working Group for City Gas Industry and Facility in the Niigataken Chuestu-oki Earthquake in Japan in 2007. Damages of City Gas Facilities in the Niigataken Chuetsu-oki Earthquake in Japan in 2007 (in Japanese). 2008.
[31] Meyersohn WD, O'Rourke TD. Pipeline Buckling Caused by Compressive Ground Failure During Earthquakes. Proc. third Japan-U.S. Work. Earthq. Resist. Des. Lifeline Facil. Countermeas. Soil Liq., Buffalo, NY: Technical Report NCEER-91-0001, NCEER; 1991, p. 489–96.
[32] Matheson I, Zhou W, Zhou J, Gailing R. An Upheaval Buckling Limit State Function for Onshore Natural Gas Pipelines. 2008 7th Int Pipeline Conf Vol 3 2008:781–91. doi:10.1115/IPC2008-64687.
[33] Wang J, Haigh SK, Forrest G, Thusyanthan NI. Mobilization distance for upheaval buckling of shallowly buried pipelines. J Pipeline Syst Eng Pract 2011;3:106–14. doi:10.1061/(ASCE)PS.1949-1204.0000099.
[34] Mitsuya M, Sakanoue T, Motohashi H. Beam-Mode Buckling of Buried Pipeline Subjected to Seismic Ground Motion. J Press Vessel Technol 2013;135:1–10. doi:10.1115/PVP2012-78559.
[35] O'Rourke TD, O'Rourke MJ. Pipeline Response to Permanent Ground Deformation: A Benchmark Case. In: Technical Council on Lifeline Earthquake Engineering, editor. Proc. Fourth U.S. Conf. Lifeline Earthq. Eng., Monograph No. 6, ASCE; 1995, p. 288–95.
[36] Kennedy RP, Darrow AC, Short SA. General considerations for seismic design of oil pipeline systems. Irvine, Calif.; Los Angeles, Calif.: Engineering Decision Analysis Co. ; Dames & Moore; 1977.
[37] Japan Gas Association. Seismic Design for Gas Pipelines 2000:91–100.
[38] European Committee for Standardization (CEN). Eurocode 8: Design of structures for earthquake resistance—Part 4: Silos,tanks and pipelines (EN 1998-4: 2006). Eur Comm Norm Brussels 2003;2.
[39] O'Rourke TD, Roth B, Miura F, Hamada M. Case History of High Pressure Pipeline Response to Liquefaction-Induced Ground Movements. Proceedings, 4th U.S. Natl. Conf. Earthq. Eng., Palm Springs, CA: 1990, p. 955–64.
[40] Brazier LG. On the Flexure of Thin Cylindrical Shells and Other "Thin" Sections. Proc R Soc London Ser A 1927;116:104 LP-114.
[41] Gresnigt A. Plastic design of buried steel pipes in settelement areas. HERON 1986;4:1–113.
[42] Moncarz P, Shyne J, Derbalian G. Failures of 108-Inch Steel Pipe Water Main. J Perform Constr Facil 1987;1:168–87. doi:10.1061/(ASCE)0887-3828(1987)1:3(168).
[43] Brockenbrough R. Strength of Bell-and-Spigot Joints. J Struct Eng 1990;116:1983–91. doi:10.1061/(ASCE)0733-9445(1990)116:7(1983).
[44] Tawfik MS, O'Rourke TD. LOAD-CARRYING CAPACITY OF WELDED SLIP JOINTS. J Press Vessel Technol Trans ASME 1985;107:36–43.
[45] Kubo K. Fundamental Concept Of Aseismic Design Of Underground Piping Systems. Proc. 5th Eur. Conf. Earthq. Engng, Istanbul, Turkey: 1975.
[46] Shinozuka BM, Kameda H, Koike T. Ground strain estimation for seismic risk analysis 1983;109:175–91.
[47] O'Rourke MJ, Hmadi K El. Analysis of continuous buried pipelines for seismic wave effects. Earthq Eng Struct Dyn 1988;16:917–29. doi:10.1002/eqe.4290160611.
[48] Hindy A, Novak M. Earthquake response of underground pipelines. Earthq Eng Struct Dymamics 1979;7:451–76.

[49] Zerva A. Pipeline Response to Directionally and Spatially Correlated Seismic Ground Motions. J Press Vessel Technol 1993;115:53–8.
[50] Katayama T. Use of dense array data in the determination of engineering properties of strong motions. Struct Saf 1991;10:27–51. doi:10.1016/0167-4730(91)90005-T.
[51] Papadopoulos SP, Sextos AG, Kwon O-S, Gerasimidis S, Deodatis G. Impact of spatial variability of earthquake ground motion on seismic demand to natural gas transmission pipelines. 16th World Conf. Earthq. Eng. Santiago, Chile, 9-13 January., 2017.
[52] Newmark NM. Problems in wave propagation in soil and rock. Proc. Int. Symp. wave Propag. Dyn. Prop. earth Mater., Albuquerque: University of New Mexico Press; 1968, p. 7–26.
[53] Kuesel TR. Earthquake Design Criteria for Subways. J Struct Div ASCE 1969.
[54] Wang JN. Seismic Design of Tunnels. A Simple State of the Art Approach 1993:1–147.
[55] St John CM, Zahrah TF. Aseismic design of underground structures. Tunn Undergr Sp Technol 1987;2:165–97. doi:10.1016/0886-7798(87)90011-3.
[56] Parmelee RA, Ludtke CA. SEISMIC SOIL-STRUCTURE INTERACTION OF BURIED PIPELINES. 1975:406–15.
[57] Audibert JME, Nyman KJ. SOIL RESTRAINT AGAINST HORIZONTAL MOTION OF PIPES. ASCE J Geotech Eng Div 1977;103:1119–42.
[58] O'Rourke M, Wang LRL. Earthquake response of buried pipelines. Spec. Conf. Earthq. Eng. Soil Dyn., Pasadena, CA: ASCE; 1978, p. 720–731.
[59] Nyman K. Soil response against oblique motion of pipes. J Transp Eng 1984;110:190–202.
[60] Trautmann CH, O'Rourke TD. Lateral force-displacement response of buried pipe. J Geotech Eng 1985;111:1077–92.
[61] Selvadurai APS. Soil-pipeline interaction during ground movement. Civ. Eng. Arct. offshore, Arct. `85, New York, N.Y.: American Society of Civil Engineers; 1985, p. 763–73.
[62] El Hmadi K, O'Rourke M. Soil Springs for Buried Pipeline Axial Motion. J Geotech Eng 1988;114:1335–9.
[63] Colton JD, International. SRI. Measurement of dynamic soil-pipe axial interaction for full-scale buried pipelines under field laying conditions. Final report. Menlo Park, Ca.: SRI International; 1981.
[64] Katsumi M, Masaru H. Soil Spring Constants of Buried Pipelines for Seismic Design. J Eng Mech 2000;126:76–83. doi:10.1061/(ASCE)0733-9399(2000)126:1(76).
[65] Hsu T, Chen Y, Wu C. Soil Friction Restraint of Oblique Pipelines in Loose Sand. J Transp Eng 2001;127:82–7. doi:10.1061/(ASCE)0733-947X(2001)127:1(82).
[66] American Lifeline Alliance. Guideline for the Design of Buried Steel Pipe. vol. 2001. 2005.
[67] Hansen JB, Christensen NH. The ultimate resistance of rigid piles against transversal forces. Copenhagen: Geoteknisk Institut; 1961.
[68] Trautmann CH, O'Rourke TD, University. C, Engineering. S of C and E, (U.S.) NSF. Behavior of pipe in dry sand under lateral and uplift loading. Ithaca, N.Y.: School of Civil and Environmental Engineering, Cornell University; 1983.
[69] Loh CH, Penzien J, Tsai YB. Engineering analyses of smart 1 array accelerograms. Earthq Eng Struct Dyn 1982;10:575–91. doi:10.1002/eqe.4290100407.
[70] Abrahamson NA, Bolt BA, Darragh RB, Penzien J, Tsai YB. The SMART I Accelerograph Array (1980-1987): A Review. Earthq Spectra 1987;3:263–87. doi:10.1193/1.1585428.
[71] Der Kiureghian A, Neuenhofer A. Response spectrum method for multi-□support seismic excitations. Earthq Eng Struct Dyn 1992;21:713–40. doi:10.1002/eqe.4290210805.
[72] Sextos AG, Pitilakis KD, Kappos AJ. Inelastic dynamic analysis of RC bridges accounting for spatial variability of ground motion, site effects and soil-structure interaction phenomena. Part 1: Methodology and analytical tools. Earthq Eng Struct Dyn 2003;32:607–27. doi:10.1002/eqe.241.
[73] Deodatis G, Shinozuka M. Simulation of Seismic Ground Motion Using Stochastic Waves. J Eng Mech 1989;115:2723–2737.
[74] Sextos AG, Kappos AJ. Evaluation of seismic response of bridges under asynchronous excitation and comparisons with Eurocode 8-2 provisions. Bull Earthq Eng 2009;7:519–45. doi:10.1007/s10518-008-9090-5.
[75] Sextos AG, Karakostas C, Lekidis V, Papadopoulos S. Multiple support seismic excitation of the Evripos bridge based on free-field and on-structure recordings. Struct Infrastruct Eng 2015;11:1510–23. doi:10.1080/15732479.2014.977302.
[76] Norman JAP, Virden DW, Crewe AJ, Wagg DJ. Physical modelling of bridges subject to multiple support excitation 2006;9:5111–20.
[77] Saiidi MS, Vosooghi A, Nelson RB. Shake-Table Studies of a Four-Span Reinforced Concrete Bridge. ASCE J Struct Eng 2013;139:1352–61. doi:10.1061/(ASCE)ST.1943-541X.0000790.
[78] Zerva A. Spatial Variation of Seismic Ground Motions: Modeling and Engineering Applications. Boca Raton, Fla.: CRC Press, Taylor & Francis Group; 2009.
[79] Zhang B, Papageorgiou AS. Simulation of the response of the marina district Basin, San Francisco, California, to the 1989 Loma Prieta earthquake. Bull Seismol Soc Am 1996;86:1382–400.
[80] Assimaki D, Kausel E, Gazetas G. Wave propagation and soil-structure interaction on a cliff crest during the 1999 Athens Earthquake. Soil Dyn Earthq Eng 2005;25:513–27. doi:10.1016/j.soildyn.2004.11.031.
[81] Psarropoulos PN, Tazoh T, Gazetas G, Apostolou M. Linear and Nonlinear Valley Amplification Effects of Seismic Ground Motion. Soils Found Japanese Geotech Soc 2007;47:857–71.
[82] Gelagoti F, Kourkoulis R, Anastasopoulos I, Tazoh T, Gazetas G. Seismic wave propagation in a very soft alluvial valley: Sensitivity to ground-motion details and soil nonlinearity, and generation of a parasitic vertical component.

Bull Seismol Soc Am 2010;100:3035–54. doi:10.1785/0120100002.
[83] Scandella L, Paolucci R. Earthquake induced ground strains in the presence of strong lateral soil heterogeneities. Bull Earthq Eng 2010;8:1527–46. doi:10.1007/s10518-010-9186-6.
[84] Nishio N, Ukaji T, Tsukamoto K. Experimental Studies and Observation of Pipeline Behavior During Earthquakes. PVP-Vol. 43, 1980, p. 67–76.
[85] Nishio N, Ishita O, Tsukamoto K. Model experiments on the behavior of buried pipelines during earthquakes. Am. Soc. Mech. Eng., Press. Vessel. Pip. Div., (Tech. Rep.) PVP; (United States), vol. PVP-VOL. 7, 1983.
[86] Akiyoshi T, Fuchida K. Seismic Resposne of Pipeline Systems Buried in Dipping Soil Layers. Proc. 9th World Conf. Earthq. Eng., Tokyo-Kyoto, Japan: 1988.
[87] Ando H, Sato S, Takagi N. Seismic Observation of a Pipeline Buried at the Heterogeneous Ground. Proc Tenth World Conf Earthq Eng 1992:5563–7.
[88] Liang J. Dynamic Response of Pipelines Laid Through Riverbeds. PVP-Vol. 312, 1995, p. 147–152.
[89] Liang J. 3-D Seismic Response of Pipelines Through Multiple Soil Media. PVP-Vol. 312, 1995, p. 101–107.
[90] Zerva A, Ang A.-S, Wen YK. A Study of Seismic Ground Motion for Lifeline Response Analysis. Civ Eng Stud Struct Res Ser (University Illinois Urbana-Champaign, Dep Civ Eng 1985.
[91] Zerva A. On the spatial variation of seismic ground motions and its effects on lifelines. Eng Struct 1994;16:534–46. doi:10.1016/0141-0296(94)90089-2.
[92] HARICHANDRAN RS, VANMARCKE EH. Stochastic Variation of Earthquake Ground Motion in Space and Time. J Eng Mech 1986;112:154–74.
[93] Luco JE, Wong HL. Response of a rigid foundation to a spatially random ground motion. Earthq Eng Struct Dyn 1986;14:891–908. doi:10.1002/eqe.4290140606.
[94] Lee D-H, Kim B-HBH, Lee H, Kong J-SJS. Seismic behavior of a buried gas pipeline under earthquake excitations. Eng Struct 2009;31:1011–23. doi:10.1016/j.engstruct.2008.12.012.
[95] Karamitros DK, Bouckovalas GD, Kouretzis GP. Stress analysis of buried steel pipelines at strike-slip fault crossings. Soil Dyn Earthq Eng 2007;27:200–11. doi:10.1016/j.soildyn.2006.08.001.
[96] Shinozuka M, Koike T. ESTIMATION OF STRUCTURAL STRAINS IN UNDERGROUND LIFELINE PIPES. 1979:31–48.
[97] Wong K, Datta S, Shah A. Three-Dimensional Motion of Buried Pipeline. I: Analysis. J Eng Mech 1986;112:1319–37. doi:10.1061/(ASCE)0733-9399(1986)112:12(1319).
[98] Wong BKC, Shah AH, Asce M. THREE-DIMENSIONAL MOTION OF BURIED PIPELINE . II : NUMERICAL RESULTS Numerical results are presented for a model simulating a concrete shell buried in a soil-like or rock-like material . The material properties of the pipe and the host materials in the ha 1987;112:1338–45.
[99] Kouretzis GP, Bouckovalas GD, Gantes CJ. 3-D shell analysis of cylindrical underground structures under seismic shear (S) wave action. Soil Dyn Earthq Eng 2006;26:909–21. doi:10.1016/j.soildyn.2006.02.002.
[100] Hatzigeorgiou GD, Beskos DE. Soil–structure interaction effects on seismic inelastic analysis of 3-D tunnels. Soil Dyn Earthq Eng 2010;30:851–61. doi:10.1016/j.soildyn.2010.03.010.
[101] Saberi M, Behnamfar F, Vafaeian M. A semi-analytical model for estimating seismic behavior of buried steel pipes at bend point under propagating waves. Bull Earthq Eng 2013;11:1373–402. doi:10.1007/s10518-013-9430-y.
[102] Nourzadeh D, S. T. Response of Gas Distribution Pipelines Network to Seismic Wave Propagation in Greater Tehran Area, Iran. 6th China-Japan-US Trilateral Symp Lifeline Earthq Eng., 2013, p. 237–44.
[103] Vazouras P, Dakoulas P, Karamanos SA. Pipe-soil interaction and pipeline performance under strike-slip fault movements. Soil Dyn Earthq Eng 2015;72:48–65. doi:10.1016/j.soildyn.2015.01.014.
[104] Vazouras P, Karamanos SA, Dakoulas P. Mechanical behavior of buried steel pipes crossing active strike-slip faults. Soil Dyn Earthq Eng 2012;41:164–80. doi:10.1016/j.soildyn.2012.05.012.
[105] Daiyan N, Kenny S, Phillips R, Popescu R. Investigating pipeline–soil interaction under axial–lateral relative movements in sand. Can Geotech J 2011;48:1683–95. doi:10.1139/t11-061.
[106] Sarvanis GC, Ferino J, Karamanos SA, Vazouras P, Dakoulas P, Mecozzi E, et al. Soil-Pipe Interaction Models for Simulating the Mechanical Response of Buried Steel Pipelines Crossing Active Faults 2016.
[107] Vazouras P, Karamanos SA. Structural behavior of buried pipe bends and their effect on pipeline response in fault crossing areas. Bull Earthq Eng 2017. doi:10.1007/s10518-017-0148-0.
[108] Chaloulos YK, Bouckovalas GD, Zervos SD, Zampas AL. Lateral soil-pipeline interaction in sand backfill: Effect of trench dimensions. Comput Geotech 2015;69:442–51. doi:10.1016/j.compgeo.2015.05.014.
[109] Chaloulos YK, Bouckovalas GD, Karamitros DK. Trench effects on lateral p-y relations for pipelines embedded in stiff soils and rocks. Comput Geotech 2017;83:52–63. doi:10.1016/j.compgeo.2016.10.018.
[110] Kouretzis GP, Sheng D, Sloan SW. Sand-pipeline-trench lateral interaction effects for shallow buried pipelines. Comput Geotech 2013;54:53–9. doi:10.1016/j.compgeo.2013.05.008.
[111] Trifonov O V., Cherniy VP. Elastoplastic stress-strain analysis of buried steel pipelines subjected to fault displacements with account for service loads. Soil Dyn Earthq Eng 2012;33:54–62. doi:10.1016/j.soildyn.2011.10.001.
[112] Bielak J, Loukakis K, Hisada Y, Yoshimura C. Domain Reduction Method for Three-Dimensional Earthquake Modeling in Localized Regions, Part I: Theory. Bull Seismol Soc Am 2003;93:817 LP-824.
[113] Rajani BB, Tesfamariam S. Uncoupled axial, flexural, and circumferential pipe-soil interaction analyses of partially supported jointed water mains. Can Geotech J 2004;41:997–1010.
[114] Paquette JA, Kyriakides S. Plastic buckling of tubes under axial compression and internal pressure. Int J Mech Sci 2006;48:855–67. doi:10.1016/j.ijmecsci.2006.03.003.
[115] NASA. NASA SP-8007 Bucking of Thin Walled Circular Cylinders. 1968. doi:19690013955.
[116] ArcelorMittal. High yield SAW welded Pipe API 5L grade X65 PSL 2 2013;65:5–6.

[117] Castro SGP, Zimmermann R, Arbelo MA, Khakimova R, Hilburger MW, Degenhardt R. Geometric imperfections and lower-bound methods used to calculate knock-down factors for axially compressed composite cylindrical shells. Thin-Walled Struct 2014;74:118–32. doi:10.1016/j.tws.2013.08.011.
[118] Shinozuka M, Koike T. Estimation of Structural Strains in Underground Lifeline Pipes. 1979.
[119] Mclaughlin P. TCLEE 2009: Lifeline Earthquake Engineering in a Multihazard Environment ©2009 ASCE 382 2009:382–92.
[120] Hamada M, O'Rourke T, Yoshizaki K. Large Deformation Behavior of Low-Angle Pipeline Elbows Subjected To In-Plane Bending. Proc 12th World Conf Earthq Eng Auckland, New Zeal 2000;Paper No.:1–8.
[121] Yoshizaki K, O'Rourke TD, Hamada M. Large Scale Experiments of Buried Steel Pipelines With Elbows Subjected To Permanent Ground Deformation. Struct Eng / Earthq Eng 2003;20:1S–11S. doi:10.2208/jsceseee.20.1s.
[122] Karamitros DK, Zoupantis C, Bouckovalas GD. Buried pipelines with bends : analytical verification against permanent ground displacements 1 2016;1793:1782–93. doi:10.1139/cgj-2016-0060.
[123] Karamanos SA. Mechanical Behavior of Steel Pipe Bends: An Overview. J Press Vessel Technol 2016;138:41203. doi:10.1115/1.4031940.
[124] Kubo K. Behavior of Underground Water pipes During an Earthquake. Proc. 5th World Conf. Earthq. Eng., Rome: 1974, p. 569–78.
[125] Ohtsuki A, Yamahara H, Tazoh T. Effect of Lateral Inhomogeneity On Seismic Waves , II . Observations and Analyses. Earthq Eng Struct Dyn 1984;12:795–816.
[126] Honegger DG, Wijewickreme D. Seismic risk assessment for oil and gas pipelines. 2013. doi:10.1533/9780857098986.4.682.
[127] Cornell CA, Krawinkler H. Progress and Challenges in Seismic Performance Assessment. PEER Cent News 3(2) 2000. http://peer.berkeley.edu/news/2000spring/performance.html (accessed July 1, 2017).
[128] Lanzano G, Salzano E, de Magistris FSFS, Fabbrocino G. Seismic vulnerability of natural gas pipelines. Reliab Eng Syst Saf 2013;117:73–80. doi:10.1016/j.ress.2013.03.019.
[129] Lanzano G, Salzano E, Santucci de Magistris F, Fabbrocino G. Seismic vulnerability of gas and liquid buried pipelines. J Loss Prev Process Ind 2013;28:72–8. doi:10.1016/j.jlp.2013.03.010.
[130] Stefanidou SP, Kappos AJ. Methodology for the development of bridge-specific fragility curves. Earthq Eng Struct Dyn 2017;46.
[131] Katayama T, Kubo K, Sato N. Earthquake damage to water and gas distribution systems. U.S. Natl. Conf. Earthq. Eng., Oakland, CA: EERI; 1975, p. 396–405.
[132] Eguchi RT. Seismic vulnerability models for underground pipes. Earthq. Behav. Saf. Oil Gas Storage Facil. Buried Pipelines Equip., New York: ASME; 1983, p. 368–73.
[133] Barenberg ME. Correlation of pipeline damage with ground motions. J Geotech Eng 1988;114:706–11. doi:10.1061/(ASCE)0733-9410(1988)114:6(706).
[134] Ballantyne DB, Berg E, Kennedy J, Reneau R, Wu D. Earthquake loss estimation modeling for the Seattle water system: Report to U.S. Geological Survey under Grant 14-08-0001-G1526. Federal Way, Wash: 1990.
[135] ASCE-TCLEE. Seismic loss estimation for a hypothetical water system. Los Angeles, California: ASCE; 1991.
[136] Hamada M. Estimation of earthquake damage to lifeline systems in Japan. 3rd Japan-U.S. Work. Earthq. Resist. Des. Lifeline Facil. Countermeas. Soil Liq. Tech. Rep. NCEER-91-0001, San Francisco: Buffalo: National Center for Earthquake Engineering Research; 1991, p. 6–22.
[137] Rourke TDO, Stewart HE, Gowdy TE, Pease JW, Gowdy TE, Pease JW. Lifeline and Geotechnical Aspects of the 1989 Lorna Prieta Earthquake. 2nd Int. Conf. Recent Adv. Geotech. Earthq. Eng. Soil Dyn., 1991.
[138] Ayala G, O'Rourke M. Effects of the 1985 Michoacan Earthquake on Water Systems and Other Buried Lifelines in Mexico. Buffalo: 1989.
[139] HAZUS-MH. Software Programme for Estimating Potential Losses from Disasters, Federal Emergency Management Agency, Washington DC. 2004.
[140] O'Rourke TD, Toprak S, Sano Y. Factors affecting water supply damage caused by the Northridge earthquake. 6th U.S. Natl. Conf. Earthq. Eng., Seattle: EERI; 1998.
[141] Trifunac MD, Todorovska MI. Northridge, California, earthquake of 1994: density of pipe breaks and surface strains. Soil Dyn Earthq Eng 1997;16:193–207. doi:10.1016/S0267-7261(96)00042-5.
[142] O'Rourke TD, Jeon S-S. Factors affecting the earthquake damage of water distribution systems. Tech Counc Lifeline Earthq Eng Monogr 1999:379–88.
[143] Fragiadakis M, Christodoulou SE, Vamvatsikos D. Reliability Assessment of Urban Water Distribution Networks Under Seismic Loads. Water Resour Manag 2013;27:3739–64. doi:10.1007/s11269-013-0378-0.
[144] American Lifelines Alliance (ALA). Seismic Fragility Formulation for Water Systems. 2001. doi:10.1007/s13398-014-0173-7.2.
[145] O'Rourke M, Deyoe E. Seismic damage to segmented buried pipe. Earthq Spectra 2004;20:1167–83. doi:10.1193/1.1808143.
[146] Jeon SS, O'Rourke TD. Northridge earthquake effects on pipelines and residential buildings. Bull Seismol Soc Am 2005;95:294–318. doi:10.1785/0120040020.
[147] Pineda-Porras O, Ordaz M. A New Seismic Intensity Parameter to Estimate Damage in Buried Pipelines due to Seismic Wave Propagation. J Earthq Eng 2007;11:773–86. doi:10.1080/13632460701242781.
[148] O'Rourke M. Analytical fragility relation for buried segmented pipe 2009;357:73. doi:10.1061/41050(357)73.
[149] O'Rourke TD, Jeon SS, Toprak S, Cubrinovski M, Hughes M, Van Ballegooy S, et al. Earthquake response of underground pipeline networks in Christchurch, NZ. Earthq Spectra 2014;30:183–204. doi:10.1193/030413EQS062M.
[150] O'Rourke M, Filipov E, Uçkan E. Towards Robust Fragility Relations for Buried Segmented Pipe in Ground Strain

Areas. Earthq Spectra 2015;31:1839–58. doi:10.1193/032311EQS076M.
[151] Melissianos VE, Vamvatsikos D, Gantes CJ. Performance Assessment of Buried Pipelines at Fault Crossings. Earthq Spectra 2016;33:122015EQS187M. doi:10.1193/122015EQS187M.
[152] Chang FK. What is Structural Health Monitoring? Boca Raton, FL: 1999.
[153] Gastineau A, Johnson T, Schultz A. Bridge Health Monitoring and Inspections–A Survey of Methods 2009.
[154] Barbian A, Beller M. In-Line Inspection of High Pressure Transmission Pipelines : State-of-the-Art and Future Trends. 18th World Conf Nondestruct Test 2012:1–21.
[155] Bradshaw AS, Mccue MT, Kim J, Nadukuru SS, Lynch J, Michalowski RL, et al. Damage detection and health monitoring of buried concrete pipelines. Predict Simul Methods Geohazard Mitig 2009:473–8.
[156] Daniele Inaudi; Branko Glisic. Long-Range Pipeline Monitoring by Distributed Fiber Optic Sensing. J Press Vessel Technol 2010;132:9. doi:DOI: 10.1115/1.3062942.
[157] Glisic B, Yao Y. Fiber optic method for health assessment of pipelines subjected to earthquake-induced ground movement. Struct Heal Monit Int J 2012;11:696–711. doi:10.1177/1475921712455683.
[158] Posey Jr. R, Johnson GA, Vohra ST, Posey Jr. ST. Strain sensing based on coherent Rayleigh scattering in an optical fibre. Electron Lett 2000;36:1688–9. doi:10.1049/el:20001200.
[159] Kikuchi K, Naito T, Okoshi T. Measurement of Raman scattering in single-mode optical fiber by optical time-domain reflectometry. Quantum Electron IEEE J 1988;24:1973–5. doi:10.1109/3.8529.
[160] Kurashima T, Horiguchi T, Tateda M. Distributed-temperature sensing using stimulated Brillouin scattering in optical silica fibers. Opt Lett 1990;15:1038.
[161] Thévenaz L, Niklès M, Fellay A, Facchini M, Robert PA. Truly distributed strain and temperature sensing using embedded optical fibers. Proc SPIE - Int Soc Opt Eng 1998;3330:301–14. doi:10.1117/12.316986.
[162] Ravet F, Zou L, Bao X, Chen L, Huang RF, Khoo HA. Detection of buckling in steel pipeline and column by the distributed Brillouin sensor. Opt Fiber Technol 2006;12:305–11. doi:10.1016/j.yofte.2005.12.002.
[163] Techniques PI. Pipeline Inspection Techniques. PetroMin Pipeliner 2013:48–52.
[164] Sextos A. ICT applications for new generation seismic design, construction and assessment of bridges. Struct Eng Int J Int Assoc Bridg Struct Eng 2014;24:173–83. doi:10.2749/101686614X13830790993726.
[165] Bruneau M, Chang SE, Eguchi RT, Lee GC, O'Rourke TD, Reinhorn AM, et al. A Framework to Quantitatively Assess and Enhance the Seismic Resilience of Communities. Earthq Spectra 2003;19:733–52. doi:10.1193/1.1623497.
[166] Cimellaro GP, Reinhorn AM, Bruneau M. Framework for analytical quantification of disaster resilience. Eng Struct 2010;32:3639–49. doi:10.1016/j.engstruct.2010.08.008.
[167] Bruneau M, Eeri M, Chang SE, Eeri M, Ronald T, Eeri M, et al. A Framework to Quantitatively Assess and Enhance the Seismic Resilience of Communities 2003;19:733–52. doi:10.1193/1.1623497.
[168] American Society of Civil Engineers (ASCE). FEMA 356 Prestandard and Commentary for the Seismic Rehabilitation of Building. Rehabilitation 2000.
[169] Bommer JJ, Crowley H. The Influence of Ground-Motion Variability in Earthquake Loss Modelling. Bull Earthq Eng 2006;4:231–48. doi:10.1007/s10518-006-9008-z.
[170] Sextos AG, Kilanitis I, Kappos AJ, Pitsiava M, Sergiadis G, Margaris V, et al. Seismic resilience assessment of the western Macedonia highway network in Greece. 6th ECCOMAS Themat Conf Comput Methods Struct Dyn Earthq Eng M Papadrakakis, M Fragiadakis Rhodes Island, Greece, June 15–17 2017.
[171] Gantes CJ, Melissianos VE. Evaluation of Seismic Protection Methods for Buried Fuel Pipelines Subjected to Fault Rupture. Front Built Environ 2016;2. doi:10.3389/fbuil.2016.00034.
[172] Melissianos VE, Korakitis GP, Gantes CJ, Bouckovalas GD. Numerical evaluation of the effectiveness of flexible joints in buried pipelines subjected to strike-slip fault rupture. Soil Dyn Earthq Eng 2016;90:395–410. doi:10.1016/j.soildyn.2016.09.012.
[173] Zulfikar C, Erdik M, Safak E, Biyikoglu H, Kariptas C. Istanbul natural gas network rapid response and risk mitigation system. Bull Earthq Eng 2016;14:2565–78. doi:10.1007/s10518-016-9964-x.
[174] Cimellaro G, Villa O, Bruneau M. Resilience-Based Design of Natural gas distribution networks. J Infrastruct Syst 2014;21:1–14. doi:10.1061/(ASCE)IS.1943-555X.0000204.
[175] Shahriar A, Sadiq R, Tesfamariam S. Risk analysis for oil & gas pipelines: A sustainability assessment approach using fuzzy based bow-tie analysis. J Loss Prev Process Ind 2012;25:505–23. doi:10.1016/j.jlp.2011.12.007.
[176] Dong Y, Frangopol DM. Risk and resilience assessment of bridges under mainshock and aftershocks incorporating uncertainties. Eng Struct 2015;83:198–208. doi:10.1016/j.engstruct.2014.10.050.
[177] American Society of Mechanical Engineers. ASME B31.4 Pipeline Transportation Systems for Liquids and Slurries 2012;2002.
[178] American Society of Mechanical Engineers. ASME B31.8: Gas Transmission and Distribution Piping Systems 2004;552. doi:10.1520/G0154-12A.